




## RESEARCH ARTICLE

# $\Delta^9$ -Tetrahydrocannabinol promotes functional remyelination in the mouse brain

Tania Aguado<sup>1,2,3</sup>  | Alba Huerga-Gómez<sup>1,2,3</sup> | Aníbal Sánchez-de la Torre<sup>1,2,3</sup> |  
 Eva Resel<sup>1,2,3</sup> | Juan Carlos Chara<sup>3,4</sup> | Carlos Matute<sup>3,4,5</sup> | Susana Mato<sup>3,4,5</sup> |  
 Ismael Galve-Roperh<sup>1,2,3</sup>  | Manuel Guzman<sup>1,2,3</sup> | Javier Palazuelos<sup>1,2,3</sup> 

<sup>1</sup>Instituto Ramón y Cajal de Investigación Sanitaria (IRYCIS), Madrid, Spain

<sup>2</sup>Department of Biochemistry and Molecular Biology, Instituto Universitario de Investigación en Neuroquímica (IUN), Complutense University, Madrid, Spain

<sup>3</sup>Centro de Investigación Biomédica en Red sobre Enfermedades Neurodegenerativas (CIBERNED), Madrid, Spain

<sup>4</sup>Department of Neurosciences, University of the Basque Country UPV/EHU and Achucarro Basque Center for Neuroscience, Leioa, Spain

<sup>5</sup>Biocruces, Barakaldo, Spain

## Correspondence

Javier Palazuelos and Tania Aguado, Department of Biochemistry and Molecular Biology, Complutense University, 28040, Madrid, Spain.  
 Email: j.palazuelos@ucm.es; taguado@ucm.es

## Funding information

Centro de Investigación Biomédica en Red sobre Enfermedades Neurodegenerativas, Grant/Award Numbers: CB06/0005/0076, CB06/05/0005; Comunidad de Madrid, Grant/Award Numbers: 2016-T1/BMD-1060, 2020-5A/BMD-19728; Basque Government (Eusko Jaurjaritza), Grant/Award Numbers: IT1203-19, PIBA19-0059; Fondation pour l'Aide à la Recherche sur la Sclérose en Plaques, ARSEP Foundation; Fundación Tatiana Pérez de Guzmán el Bueno; FEDER and Instituto de Salud Carlos III, Grant/Award Numbers: PI18-00941, PI18/00513; Ministerio de Economía y Competitividad, Grant/Award

**Background and purpose:** Research on demyelinating disorders aims to find novel molecules that are able to induce oligodendrocyte precursor cell differentiation to promote central nervous system remyelination and functional recovery.  $\Delta^9$ -Tetrahydrocannabinol (THC), the most prominent active constituent of the hemp plant *Cannabis sativa*, confers neuroprotection in animal models of demyelination. However, the possible effect of THC on myelin repair has never been studied.

**Experimental approach:** By using oligodendroglia-specific reporter mouse lines in combination with two models of toxin-induced demyelination, we analysed the effect of THC on the processes of oligodendrocyte regeneration and functional remyelination.

**Key results:** We show that THC administration enhanced oligodendrocyte regeneration, white matter remyelination and motor function recovery. THC also promoted axonal remyelination in organotypic cerebellar cultures. THC remyelinating action relied on the induction of oligodendrocyte precursor differentiation upon cell cycle exit and via CB<sub>1</sub> cannabinoid receptor activation.

**Conclusions and implications:** Overall, our study identifies THC administration as a promising pharmacological strategy aimed to promote functional CNS remyelination in demyelinating disorders.

## KEYWORDS

cannabinoids, CB<sub>1</sub> cannabinoid receptor, demyelinating disorders, mTORC<sub>1</sub>, oligodendrocyte precursor cells, remyelination, THC

**Abbreviations:** Ai6, RosaAi6(B6.Cg-Gt (ROSA)26Sor<sup>tm6(CAG-ZsGreen1)Hze/J</sup>); BrdU, 5-bromo-2'-deoxyuridine; CBD, [cannabidiol](#); Cpz, cuprizone; CC1, APC, anti-adenomatous polyposis coli; CNP, 2'-3'-cyclic nucleotide 3'-phosphodiesterase; GST $\pi$ , glutathione-S-transferase; mTORC<sub>1</sub>, mammalian target of rapamycin complex 1; NG2, neural/glial antigen 2; Olig2, oligodendrocyte transcription factor 2; THC,  $\Delta^9$ -tetrahydrocannabinol.

Tania Aguado and Alba Huerga-Gómez are equally contributing authors.

This is an open access article under the terms of the Creative Commons Attribution-NonCommercial-NoDerivs License, which permits use and distribution in any medium, provided the original work is properly cited, the use is non-commercial and no modifications or adaptations are made.

© 2021 The Authors. *British Journal of Pharmacology* published by John Wiley & Sons Ltd on behalf of British Pharmacological Society.

Numbers: PID2020-112640RB-I00, RTI2018-095311-B-I00, SAF2016-75292-R, SAF2017-83516

## 1 | INTRODUCTION

Damage to the myelin sheath is a common hallmark of demyelinating disorders such as multiple sclerosis (MS). Loss of myelin ultimately leads to a reduction of nerve conduction velocity, a phenomenon that underpins the progressive neurological decline associated with the deterioration caused by this disease (Micu et al., 2018; Morrison et al., 2013). Throughout life, by activation, recruitment and differentiation of adult oligodendrocyte precursor cells, which eventually become new myelin-forming oligodendrocytes, demyelinated axons can be repaired, thus restoring saltatory conduction and resolving functional deficits (Dubois-Dalq et al., 2008; Franklin & Ffrench-Constant, 2008; Gibson et al., 2014; Zhang et al., 2015). Remyelination confers not only neuroprotection, which is crucial for limiting axon degeneration and progressive disability, but also tissue regeneration and functional recovery (Cunniffe & Coles, 2019; Gallo & Armstrong, 2008). However, in demyelinating disorders and specifically in multiple sclerosis the immune and inflammatory response to injury limits the regenerative potential of oligodendrocyte precursor cells (Franklin & Ffrench-Constant, 2017; Miron, 2017). Hence, the failure to differentiate into mature myelinating oligodendrocytes ultimately limits axon remyelination, leading to progressive axonopathy, neurodegeneration and disability. Therefore, the identification of molecules able to directly target oligodendrocytes and promote their full development into mature myelinating oligodendrocytes is paramount to the design of therapies that induce efficient remyelination in demyelinating disorders (Cunniffe & Coles, 2019; Franklin & Ffrench-Constant, 2017; Gallo & Armstrong, 2008).

In the last years, the use of cannabis-derived molecules and extracts has emerged as a promising therapeutic strategy for the treatment of multiple sclerosis and other neuroinflammatory disorders. Thus, several clinical trials have revealed beneficial effects of phytocannabinoids in multiple sclerosis patients, relieving hallmark symptoms such as spasticity, tremor, bladder dysfunction and neuropathic pain (Messina et al., 2017; Russo, 2011; Wade et al., 2003). These studies have led to the approval of the cannabinoid-based medicine nabiximols (Sativex<sup>®</sup>), a 1:1 mixture of the two main phytocannabinoids,  $\Delta^9$ -tetrahydrocannabinol (THC) and cannabidiol (CBD), that nowadays is being prescribed in many countries worldwide for the management of multiple sclerosis-associated symptoms (Maccarrone et al., 2017). Moreover, the prescription of standardized cannabis preparations is largely increasing worldwide among multiple sclerosis patients, for example Canada, Israel, Uruguay and about half of the states of the USA (Cofield et al., 2017; Hildebrand et al., 2020; Messina et al., 2017).

Despite this widespread medicinal use, the precise mechanisms of cannabinoid action mediating the aforementioned beneficial effects

### What is already known

- $\Delta^9$ -Tetrahydrocannabinol (THC) confers neuroprotection in animal models of demyelination.

### What does this study add

- THC administration following cuprizone-induced demyelination enhanced oligodendrocyte regeneration, white matter remyelination and motor function recovery.

### What is the clinical significance

- THC administration is a promising pharmacological strategy to promote functional CNS remyelination in demyelinating disorders.

in multiple sclerosis patients are not completely understood. Numerous studies in multiple sclerosis animal models have reported a neuroprotective effect of phytocannabinoids (Croxford et al., 2008). Thus, both THC and CBD, when administered either separately or in combination, promote neuroprotection and slow down experimental autoimmune encephalomyelitis (EAE)-associated disability in mice (Al-Ghezi et al., 2019; Gonzalez-Garcia et al., 2017; Lyman et al., 1989; Wirguin et al., 1994). These actions are believed to be due to (i), **CB<sub>1</sub> receptor** activation on neurons and oligodendrocytes, promoting neural cell survival in a cell-autonomous manner (Bernal-Chico et al., 2015; Croxford et al., 2008; Maresz et al., 2007; Pryce et al., 2003) and (ii), **CB<sub>2</sub> receptor** activation on brain-resident microglia and infiltrating peripheral immune cells, promoting neural cell survival in a non-cell-autonomous manner (Eljaschewitsch et al., 2006; Maresz et al., 2007; Palazuelos et al., 2008). Strikingly, although functional myelin repair conceivably should stand as a pivotal target of any multiple sclerosis progression-attenuating therapeutic approach, the potential impact of phytocannabinoids on the process of oligodendrocyte regeneration and CNS remyelination in multiple sclerosis animal models has never been studied. Here, by using oligodendroglia-specific reporter mouse lines in combination with models of toxin-induced demyelination, we found that THC administration following demyelination promotes oligodendrocyte regeneration, CNS remyelination and motor function recovery in mice. Therefore, our study unveils an unprecedented potential of cannabinoid-based therapies for promoting oligodendrocyte regeneration and myelin repair in demyelinating disorders.

## 2 | METHODS

### 2.1 | Animal procedures

All the experimental procedures used were ethically reviewed and approved and were performed under the guidelines and with the approval of the Animal Welfare Committee of Universidad Complutense de Madrid and Comunidad de Madrid, authorization number PROEX 150/17 under the directives of the European Commission (Directive 2010/63/EU). In addition, all experimental procedures are also reported in compliance with the ARRIVE guidelines (Percie du Sert et al., 2020) and with the recommendations made by the *British Journal of Pharmacology* (Kilkenny et al., 2010). All animals used were bred into C57BL/6J background. Animals were housed, three in a cage, in temperature-controlled rooms on an artificial 12-h light/dark cycle at 22°C–24°C and relative humidity of 50%–60%, with water, food availability *ad libitum* and sterile cardboard tubes as a housing refinement. All mice were pathogen free. The cuprizone (Cpz) diet was changed daily and mice were monitored daily. The mouse lines used from Jackson Laboratories are the following:- CNP-mEGFP (Cnp-EGFP\* 1Qrlu/J, RRID: IMSR\_JAX:026105) (Deng et al., 2014), Ng2-dsRed (NG2-dsRed, Cspg4-DsRed.T1 1Akik/J Cat# RRID:IMSR\_JAX:008241) (Zhu et al., 2008), Ng2-CreER<sup>tm</sup> (NG2-Cre, Cspg4-Cre/Esr1\* BAKik/J, RRID: IMSR\_JAX:008538) (Zhu et al., 2008), and RosaAi6(B6.Cg-Gt (ROSA) 26Sor<sup>tm6(CAG-ZsGreen1)Hze/J</sup>, RRID:IMSR\_JAX:007906) (Madisen et al., 2010). By crossing the Ng2-CreER<sup>tm</sup> with the Ai6 mouse line, we generated the Ng2-CreER<sup>tm</sup>:Rosa-Ai6 mouse line (referred to as Ng2-Cre:Ai6).

### 2.2 | Materials

The dose of 3 mg·kg<sup>-1</sup> of THC used in this study is commonly used in preclinical and clinical settings. In preclinical models, this dose has been shown to exert therapeutic effects in many different settings without having undesired psychoactive effects (Long et al., 2010; Metna-Laurent et al., 2017). THC, **rimonabant (SR141716)**, 2 mg·kg<sup>-1</sup>, **SR144528** (2 mg·kg<sup>-1</sup>) or vehicle (Veh) were dissolved in Tween-80/NaCl (1:18, v/v) and 1% (v/v) of dimethyl sulfoxide as previously described (Huerga-Gomez et al., 2020). The rapamycin analogue **temsirrolimus** (5 mg·kg<sup>-1</sup>) was dissolved in 0.9% NaCl. All drugs were administered intraperitoneally (i.p.) in a volume of 10 ml·kg<sup>-1</sup> and rimonabant, **SR144528** or temsirrolimus were administered 30 min before THC administration, once a day for five consecutive days. To label proliferating cells, 5-bromo-2-deoxyuridine (BrdU, 100 mg·kg<sup>-1</sup> body weight, Sigma) was injected intraperitoneally as described previously (Palazuelos et al., 2014). To assay for cell cycle exit (Ki67/BrdU ratios), BrdU was injected three times a day, 2 h apart, followed by THC or Veh administration, and the tissue was analysed 48 h later. All experiments were performed in male adult mice (8-week-old,

20- to 25-g body weight). Mice were intracardially perfused or decapitated under deep anaesthesia (5% isoflurane). Recombination was induced following demyelination by three consecutive injections of **tamoxifen** (24 h apart; 75 mg·kg<sup>-1</sup> i.p. dissolved in sunflower oil) starting the day before Cpz diet removal. Recombination efficiency in Ng2-Cre:Ai6 mouse line was quantified by immunofluorescence analysis of the corpus callosum at 5 days after the first tamoxifen administration. We found Ai6 expression in 83.4 ± 5.1% of Olig2<sup>+</sup> cells.

### 2.3 | Cuprizone (Cpz)-induced demyelination

Six- to eight-week-old male mice were fed with a pelleted diet containing 0.2% Cpz (Bis(cyclohexanone)oxaldihydrazone); 0.2% TD.140804 (Envigo) (Palazuelos et al., 2015) for 6 weeks to induce demyelination. Then, mice were returned to regular chow for allowing remyelination. We observed similar levels of demyelination in all mouse lines analysed.

### 2.4 | Organotypic cerebellar

Slice cultures were prepared using brain tissue isolated from P8 c57/bl6 or CNP-mEGFP animals as described previously (Zhang et al., 2011). Briefly, mouse pups were decapitated, and their brains were dissected into ice-cold Hank's Balanced Salt Solution (HBSS). Three-hundred-micrometre sagittal slices of the cerebellum were cut with a tissue chopper. The slices were placed on Millicell culture inserts with 0.45-µm pore size (Millipore) in a medium containing 50% Minimal Essential Medium with Earle's salts, 25% HBSS, 25% horse serum, 25-mM HEPES buffer, UltraGlutamine, penicillin-streptomycin, amphotericin B and 5 mg·ml<sup>-1</sup> glucose. For remyelination studies, at 7 days *in vitro* slices were treated with **lyssolecithin** (lysophosphatidylcholine, Sigma-Aldrich) for 15–17 h, followed by dimethyl sulfoxide (DMSO) or THC 1-µM addition for 4 days. The medium was changed every 2 days. Slices were fixed with 4% (wt/vol) paraformaldehyde (PFA) for 30 min.

### 2.5 | Immunofluorescence

For immunohistochemistry, brain tissue was processed as previously described (Palazuelos et al., 2015). Briefly, mice were perfused transcardially with 4% PFA, and brains postfixed overnight in 4% PFA and treated with 30% sucrose before freezing. Then, 30-µm-thick coronal free-floating brain cryosections were washed in phosphate-buffered saline (PBS), blocked with PBS 0.25% Triton-X100, 10% goat serum, and incubated with the indicated primary antibodies (overnight at 4°C). Antigen retrieval for oligodendrocyte transcription factor 2 (Olig2) and Ki67 immunostainings was performed with citric acid (10 mM, pH 6, 65°C for 30 min), and for

BrdU immunostaining with HCl (2 N, 37°C 30 min), followed by boric acid (0.1 M pH 8.9, 20 min). The following day, sections were washed, and fluorescent secondary antibodies were used. Immunocytochemistry of organotypic cerebellum slices was performed by fixation in 4% PFA for 30 min on ice, then washed in PBS and blocked in PBS, 0.5% Triton-X100 and 10% goat serum, and then incubated with primary antibodies for 48 h at 4°C. Subsequently, slices were incubated with the appropriate secondary antibodies for 4 h at room temperature. To visualize cell nuclei, slices were incubated with 4',6-diamidino-2-phenylindole (DAPI) for 5 min, washed with PBS and mounted with Mowiol. The primary antibodies used are as follows: anti-CC1 (1:400, Millipore, Cat#OP80, RRID:AB\_2057371), anti-oligodendrocyte transcription factor 2 (Olig2) (1:250, Millipore Cat#AB9610, RRID:AB\_570666), anti-GST $\pi$  (1:200, MBL International Cat#312, RRID:AB\_591792), anti-myelin basic protein (1:1000, BioLegend, Cat#836504, RRID:AB\_2616694), anti-myelin oligodendrocyte glycoprotein (1:500, Abcam Cat#ab32760, RRID:AB\_2145529), anti NF-200 (1:200, Sigma Aldrich Cat#N4142, RRID:AB\_477272), anti-BrdU (1:200, Abcam Cat#ab6326, RRID:AB\_305426), anti-Ki67 (1:400, Thermo Fisher Scientific Cat#RM-9106-S0, RRID:AB\_2341197) and anti-pS6 (Ser240/244, 1:800, Cell Signaling Technology, Cat#5364, RRID:AB\_10694233). The appropriate mouse, rat and rabbit highly cross-adsorbed Alexa Fluor 488, 547 and 647 secondary antibodies (1:1000, Invitrogen) were used.

## 2.6 | Confocal microscopy

Optical sections ( $z = 0.5 \mu\text{m}$ ) of confocal epifluorescence images were sequentially acquired using a confocal laser-scanning microscope TCS-SP8 (20 $\times$ , 40 $\times$  and 63 $\times$ , Leica DMI6000 B instrument) and Leica Application Suite X (LAS X) software. All digital images were acquired in the corpus callosum of each animal, a minimum of six correlative slices from a 1-in-10 series located between +0.7 and -0.5 mm from bregma were analysed. Cell counts were performed blindly using ImageJ software [National Institutes of Health (NIH), RRID:SCR\_003070] in the corpus callosum and data are presented as the mean cell number per mm<sup>2</sup> or as a percentage of positive cells. When counting the percentage of Olig2<sup>+</sup> cells that expressed either NG2-dsRed or CC1, only NG2-dsRed<sup>+</sup>CC1<sup>neg</sup> and NG2-dsRed<sup>neg</sup>CC1<sup>+</sup> cells were included. Double positive NG2-dsRed<sup>+</sup>/CC1<sup>+</sup> cells were excluded from quantifications. For quantification of organotypic cultures, confocal microscopy was used to obtain stacks of images of myelin basic protein and NF200 immunolabelling in white matter areas. For analysing remyelination, Z-stack images (40 $\times$ /1.3 oil objective, optical section 1.039  $\mu\text{m}$ ) were collected from central layers within the slice. myelin basic protein<sup>+</sup> area was quantified in single stacks. Then, Z-stacks were projected onto a single plane via orthogonal projection with maximum intensity, by using LAS X imaging software, which is shown in the representative images. Three to five slices per condition and two to three fields were imaged from each slice. Three independent experiments were analysed.

## 2.7 | Electron microscopy

Mice were anesthetized with tribromoethanol (Avertin, 0.2 ml per 10 g body weight; Sigma-Aldrich) and transcardially perfused with PBS (pH 7.4) followed by a fixative solution containing 4% PFA, 2.5% glutaraldehyde and 0.5% NaCl in 0.1 M of PB, as described (Mobius et al., 2010). After extraction, brains were postfixed overnight at 4°C in fixative solution and stored in 1% PFA until use. Vibratome sections (100  $\mu\text{m}$  thick) containing the corpus callosum were cut in the coronal plane on a vibratome (VT1000S, Leica, Wetzlar, Germany). Sections were incubated in 1% OsO<sub>4</sub> for 30 min, dehydrated, embedded in epoxy resin overnight and allowed to polymerize at 60°C for 2 days. Selected tissue portions were trimmed and glued onto epoxy resin capsules. Semi-thin sections (500 nm thick) were cut using a Power Tome ultramicrotome (RMC Boeckeler, Tucson, AZ, USA) and stained with 1% toluidine blue. Ultra-thin (50–60 nm thick) sections were then cut with a diamond knife (Diatome, Hatfield PA, USA), collected on nickel mesh grids and stained with 4% uranyl acetate for 30 min and 2.5% lead citrate for electron microscope visualization. Electron microscopy images of the rostral corpus callosum located between +0.7 and -0.5 mm from bregma were taken from randomly selected fields with a Jeol JEM 1400 Plus electron microscope at the Service of Analytical and High-Resolution Microscopy in Biomedicine of University of the Basque Country UPV/EHU. The g-ratios were analysed in 10 non-serial electron micrographs per animal taken systematically at a magnification of 5000 $\times$ . For g-ratio analysis, a minimum of 100 axons per mouse was randomly selected by placing a grid onto images and measured using Image-J software. The g-ratios were calculated as the fraction between axon diameter and the diameter of the axon plus myelin unit. Fibres with prominent unfoldings in the plane of the section were excluded.

## 2.8 | Sudan black

Floating sections were mounted on to TESPA-coated glass slides. After air drying, sections were dehydrated in 70% ethanol and stained with 0.5% Sudan black in 70% ethanol for 30 min. Excess staining was removed by washing the slides in 70% ethanol and finally rinsed with water. Samples were observed under light microscopy in a Zeiss AxioPlan2 microscope.

## 2.9 | Western blot

Corpus callosum was micro-dissected from 500- $\mu\text{m}$ -thick coronal sections, and proteins were extracted using radioimmunoprecipitation assay (RIPA) buffer (SDS 0.1%, sodium deoxycholate 0.5%, NP40 1%, NaCl 150 mM, Tris-HCl 50 mM pH 8 in PBS) containing PMSF, protease inhibitors, and sodium orthovanadate. Protein samples (2–5  $\mu\text{g}$ ) were separated on 12% acrylamide (Bio-Rad) gels and transferred to polyvinylidene difluoride (PVDF) membranes (Millipore). Membranes were placed in blocking buffer (5% w/v milk in PBS) and probed with primary antibodies overnight at 4°C. The



primary antibodies used are as follows:- anti-myelin-associated glycoprotein (1:2000, Abcam, Cat#ab89780, RRID:AB\_2042411), anti-myelin oligodendrocyte glycoprotein (1:2000, Abcam Cat#ab32760, RRID:AB\_2145529), anti-myelin basic protein (1:1000, BioLegend, Cat#836504, RRID:AB\_2616694), anti-proteolipid protein (1:2,000, Abcam, Cat#ab28486, RRID:AB\_776593) and anti- $\alpha$ -tubulin (1:5000, Sigma-Aldrich, Cat#T9026, RRID:AB\_477593). After incubation with corresponding HRP-conjugated secondary antibodies, proteins were visualized using an enhanced chemiluminescence substrate mixture (ECL Plus; GE Healthcare; Santa Cruz Biotechnology; 1:5000). Band intensity of films was quantified using Adobe Photoshop software (RRID:SCR\_014199). Protein levels were normalized to the internal control  $\alpha$ -tubulin. The Immuno-related procedures used comply with the recommendations made by the *British Journal of Pharmacology* (Alexander et al., 2018).

## 2.10 | Behavioural assessments

All tests were conducted during the light cycle, with uniform lighting conditions and white noise in an isolated room. Animals were acclimated to the room for 45–60 min before testing.

### 2.10.1 | Rotarod

To assess motor function and gross coordination, Rotarod (LE8205, Harvard Apparatus) test was adopted from Bolcskei et al. (2018) and Palazuelos et al. (2009), using a 30-mm rod with an acceleration of 4 to 40 rpm over 5 min. Briefly, mice were trained three times a day for three consecutive days, the first week after weaning, with a 30-min rest interval between trials. At adult ages, following Cpz-induced demyelination, the rotarod test was assessed three times on the day of analysis during remyelination. The latency to fall off the rod was measured, with a maximum recording time of 300 s.

### 2.10.2 | Beam walking test

To evaluate fine motor coordination, mice were trained to cross a narrow wood beam (100 cm length, 10 mm width) to reach a safety box. The time to cross the beam was measured in two consecutive tests (Skripuletz et al., 2010).

### 2.10.3 | Open-field test

Mice were placed in the centre of an open-field arena (70 × 70 × 40 cm) and allowed to freely explore it for 10 min. Their behaviour was recorded by a video camera placed above and the video tracking software SMART 3.0 (Panlab, Spain, RRID: SCR\_002852) was used for video analysis. Total distance travelled (cm) was used as a measure of locomotor activity,

whereas the number of entries in the central area of the arena was used as a parameter of anxiety-linked behaviours (Prut & Belzung, 2003).

## 2.11 | Data and analysis

Data and statistical analysis comply with the recommendations of the *British Journal of Pharmacology* on experimental design and analysis in pharmacology (Curtis et al., 2018). The number of animals per group or experiments per condition ( $n$ ) is indicated in every case. The declared group size is the number of independent values and that statistical analysis was done using these independent values. Studies were designed to generate groups of equal size, using randomization and blinded analysis. The numbers illustrated represent the animals used in each of the experiments, after considering any unexpected loss of data or exclusion criterion. In some cases, experimental losses may be determined by animals receiving the wrong treatment, infections unrelated to the experiment, sampling errors (e.g. inadequate calibration of equipment & software error during acquisition) or other human error (e.g. forgetting to switch on equipment). Power analysis was conducted with IBM SPSS software (IBM France, Bois-Colombes, France RRID:SCR\_002865). Statistical analysis was undertaken only for experiments with a sample size of at least  $n = 5$  per group. For electron microscopy and some western blot experiments presented with a smaller sample size  $n < 5$ , data are presented as preliminary or exploratory observations. All variables were first tested for both, normality (Shapiro test or D'Agostino & Pearson normality test with  $P > 0.05$ ) and homogeneity of variances (Brown–Forsythe test with  $P > 0.05$ ). When comparing two groups, we use unpaired two-tailed  $t$  test for normal distribution (Student's unpaired  $t$ -tests were Welch-corrected if needed) or Mann–Whitney test when they did not distribute normally. For comparisons of more than two groups, if data were found to be normally distributed, one-way analysis of variance (ANOVA) followed by Tukey's post hoc test or uncorrected Fisher's LSD when appropriate, was carried out. The post hoc tests were conducted only if  $F$  in ANOVA achieved  $P < 0.05$ , and there was no significant variance inhomogeneity. If data were found to not be normally distributed, then a Kruskal–Wallis one-way ANOVA with uncorrected Dunn's post hoc test was carried out. Outliers were not excluded from data analysis. Differences with  $P < 0.05$  between group means were considered statistically significant. All data analyses were done using GraphPad Prism 7.00 (RRID: SCR\_002798).

## 2.12 | Nomenclature of targets and ligands

Key protein targets and ligands in this article are hyperlinked to corresponding entries in the IUPHAR/BPS Guide to PHARMACOLOGY <http://www.guidetopharmacology.org> and are permanently archived in the Concise Guide to PHARMACOLOGY 2019/20 (Alexander et al., 2019).

### 3 | RESULTS

#### 3.1 | THC promotes CNS remyelination

To evaluate the effect of THC on myelin repair under demyelinating conditions, we first used the Cpz animal model of demyelination. Wild-type mice were fed with a 0.2% Cpz diet for 6 weeks to induce global demyelination, followed by a regular diet to allow for spontaneous remyelination. The day after Cpz removal, THC (3 mg·kg<sup>-1</sup>, i.p.) or Veh was administered for five consecutive days and remyelination was analysed in the corpus callosum (Figure 1a). Western blot analysis of dissected corpus callosum extracts revealed the nearly complete demyelination achieved by the Cpz diet compared with the regular chow diet. This was assessed by quantification of the levels of myelin-related proteins, such as myelin-associated glycoprotein, myelin oligodendrocyte glycoprotein and myelin basic protein (Figure 1b). Preliminary analysis of samples obtained during the recovery phase showed an enhancement of remyelination in THC-treated mice, with increased levels of myelin-associated proteins compared with Veh-treated mice (Figure 1b). Sudan black (Figure 1c) staining further supported that THC-treated mice had increased myelin levels in the corpus callosum when compared with Veh-treated mice during remyelination. Exploratory ultrastructural analysis by electron microscopy in the corpus callosum revealed a reduced g-ratio in THC-treated mice when compared with controls (Figure 1d), therefore indicating an increased myelin thickness and confirming the THC-enhanced remyelination in the corpus callosum.

To further expand the aforementioned Cpz-derived data, we used the lysophosphatidylcholine (lysolecithin) toxin model of demyelination in organotypic cerebellar cultures from the *CNP-mEGFP* mice reporter mouse line (Deng et al., 2014), in which membrane-anchored green fluorescent protein (eGFP) expression is driven by the 2'-3'-cyclic nucleotide 3'-phosphodiesterase (CNP) promoter and found in the differentiated myelinating cell lineage. Demyelination was induced by lysolecithin treatment for 16 h, and remyelination was analysed in the presence of THC (1 μM) or Veh. Immunofluorescence analysis revealed increased myelin basic protein<sup>+</sup> area in the cerebellar white matter of THC-treated slices compared with Veh-treated controls (Figure 1e). Taken together, all these observations support that THC exposure following demyelination enhances remyelination in the mouse CNS.

#### 3.2 | THC enhances functional recovery during remyelination

The Cpz model induces nearly complete demyelination in multiple brain regions that was accompanied by various behavioural alterations that mirrored closely the clinical symptomatology of multiple sclerosis (Franco-Pons et al., 2007; Serra-de-Oliveira et al., 2015; Xu et al., 2009). Furthermore, during the recovery period, spontaneous remyelination is translated into functional recovery (Duncan et al., 2009; Ishii et al., 2019), with a progressive improvement in the

behavioural deficits, mostly observed at the motor level (Han et al., 2020; Morell et al., 1998; Templeton et al., 2019). Hence, we next analysed whether the enhancement in CNS remyelination upon THC administration was reflected in improved functional recovery. Behavioural tests were performed at Days 5 and 15 of the remyelination period in mice treated with Veh or THC for five consecutive days (Figure 2). Cpz diet-induced demyelination was accompanied by remarkable motor impairment, as evidenced by a reduced latency to fall in the *rotarod* test (Figure 2a), an increased crossing time in the *beam walk* test (Figure 2b) and a reduced distance travelled in the *open-field* test (Figure 2c). Cpz diet also increased anxiety-like behaviours, as evidenced by a reduced number of entries in the centre of the arena in the open-field test (Figure 2c). Following Cpz removal, upon remyelination, THC-treated mice showed an improved motor function in the rotarod (Figure 2a), beam walking (Figure 2b) and open-field tests (Figure 2c) compared with Veh-treated animals. These data support that THC administration promotes CNS remyelination and motor function recovery in a concerted manner.

#### 3.3 | THC promotes oligodendrocyte progenitor cell differentiation and oligodendrocyte regeneration

CNS remyelination relies on the differentiation of oligodendrocyte precursor cells into premyelinating oligodendrocytes, which contact demyelinated axons and differentiate in turn into mature, myelinating oligodendrocytes capable of forming functional myelin sheaths that contribute to neuronal protection and functionality (Chari, 2007; Cunniffe & Coles, 2019; Franklin & Ffrench-Constant, 2017). To evaluate whether the observed THC-enhanced remyelination results from a greater generation of new oligodendrocytes, we monitored oligodendrocyte loss and regeneration in the corpus callosum at the demyelination and remyelination periods. Immunofluorescence analysis revealed that the Cpz diet reduced CC1<sup>+</sup> oligodendrocytes density, down to a 20.3 ± 2.6% of the regular diet (Figure 3a,b). We also found a higher density of CC1<sup>+</sup> oligodendrocytes in the corpus callosum of THC-treated mice during the recovery phase compared with controls (Figure 3a,b). Differentiation-state analysis of the oligodendrocyte population revealed a higher percentage of CC1<sup>+</sup> oligodendrocytes within the Olig2<sup>+</sup> cell population in THC-treated mice as compared with controls (Figure 3b), indicating a higher oligodendrocyte differentiation. No difference was observed in the total number of Olig2<sup>+</sup> cells between THC and Veh-treated mice (Figure S1a), suggesting that THC induces oligodendrocyte progenitor cell differentiation during remyelination without affecting oligodendrocyte lineage survival.

We next analysed whether THC administration enhances the generation of mature myelinating oligodendrocytes. Immunofluorescence analysis and quantification of GSTπ<sup>+</sup> (glutathione-S-transferase π) cells in the corpus callosum revealed a higher density of GSTπ<sup>+</sup> mature oligodendrocytes in THC-treated mice compared with controls during remyelination (Figure 3c). To further study oligodendrocyte regeneration, we used the *CNP-mEGFP* reporter mouse line (Deng

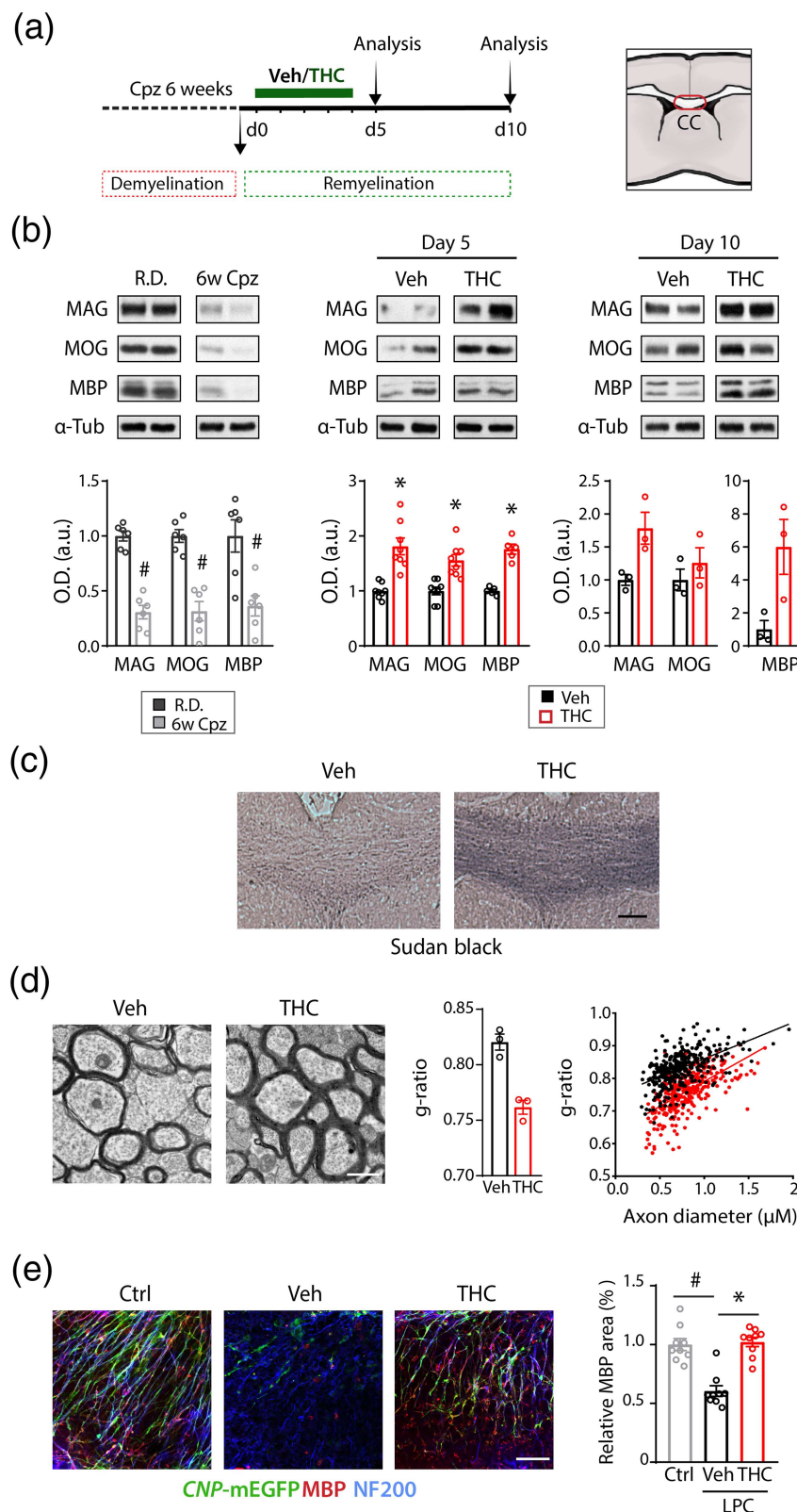


**FIGURE 1**  $\Delta^9$ -Tetrahydrocannabinol (THC) enhances CNS remyelination. (a) Left diagram represents the timeline of treatments and time points of analysis. Mice were fed with a cuprizone (Cpz) diet for 6 weeks and returned to regular diet for allowing remyelination. At 24 h after Cpz removal, THC ( $3 \text{ mg}\cdot\text{kg}^{-1}$ ) or vehicle (Veh) was administered for five consecutive days and mice were killed at 5 and 10 days following the first THC administration. Some control animals were fed with regular diet (R.D.) or Cpz 6 weeks (6w). Right diagram, the area of analysis within the corpus callosum (CC) is labelled in red.

(b) Representative scans of western blot analysis of myelin-associated proteins of corpus CC extracts. Optical densities values are relative to those of loading controls and expressed as arbitrary units (a.u.). (c) Representative images of Sudan black staining in the CC at Day 5 of recovery. (d) Representative electron microscopy images of axonal myelination in the CC at Day 5 of recovery. Quantitative analysis of myelin g-ratio and scatter plots of g-ratio versus axon diameter. (e) Slices were incubated with THC or Veh after lyssolecithin (LPC)-induced demyelination. Representative confocal images of Z-stack projection of CNP-mEGFP (green), myelin basic protein (MBP; red) and NF200 (blue) immunoreactivities in non-LPC-treated and THC or vehicle-LPC-treated cerebellar organotypic slice cultures. MBP<sup>+</sup> area was quantified in single stacks. Representative images of Z-stacks projected onto a single plane via orthogonal projection with maximum intensity. Data are shown as mean  $\pm$  SEM;  $n = 6$  (b, left panel),  $n = 8$  for MAG and myelin oligodendrocyte glycoprotein (MOG),  $n = 5$  for MBP (b, middle panel),  $n = 3$  (b, right panel);  $n = 5$  (c);  $n = 3$  (d);  $n = 9$  (e). \* $P < 0.05$  versus vehicle-treated groups or # $P < 0.05$  versus R.D., by unpaired Student's *t*-test or unpaired *t*-tests with Welch correction for MAG values (central panel) (b); \* $P < 0.05$  versus vehicle-treated group or # $P < 0.05$  versus control group by one-way ANOVA with Tukey's post hoc test (e). Scale bars (c) = 70  $\mu\text{m}$ , (d) = 4  $\mu\text{m}$ , (e) = 50  $\mu\text{m}$

et al., 2014). Thus, CNP-mEGFP mice that were treated with THC during the remyelination phase showed increased mEGFP fluorescence intensity in the corpus callosum compared with their Veh-treated littermates (Figure S1b). Together, all these data indicate that THC administration following demyelination promotes the

regeneration of fully myelinating oligodendrocytes, thereby promoting functional CNS remyelination.

To provide further support to the concept that the THC-evoked modulation of oligodendrocyte regeneration and CNS remyelination occurs at the expense of oligodendrocyte progenitor cell cycle arrest



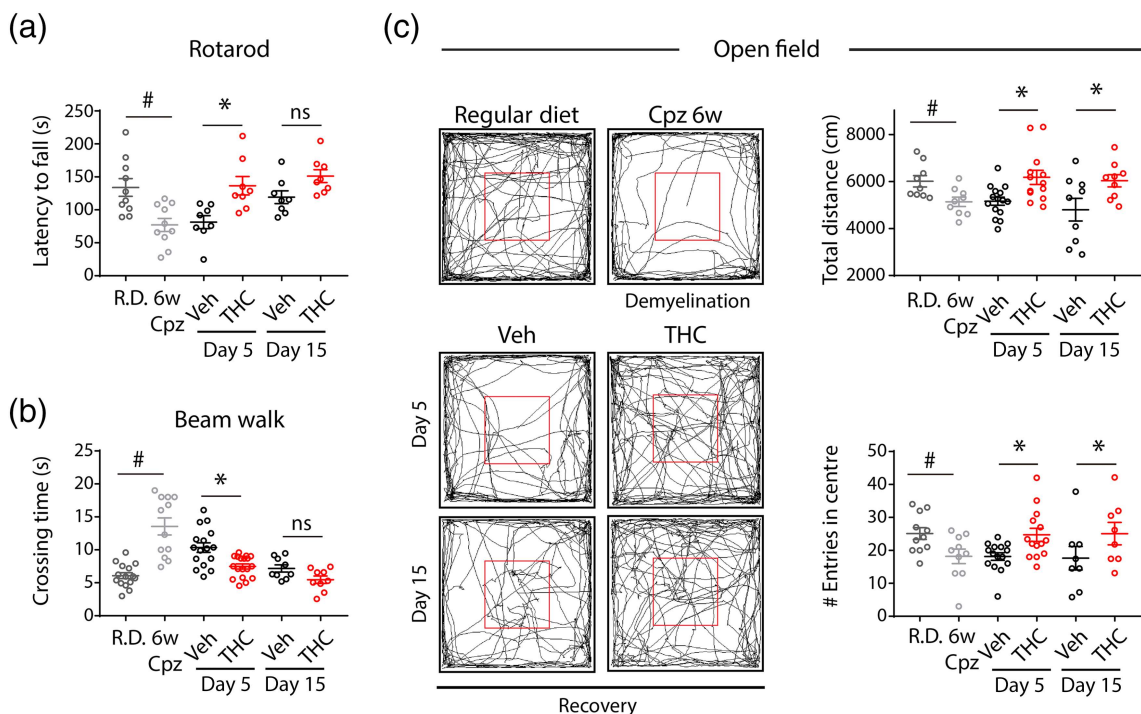


**FIGURE 2**  $\Delta^9$ -Tetrahydrocannabinol (THC) enhances functional recovery during remyelination. Mice were fed with a 0.2% cuprizone (Cpz) diet for 6 weeks, followed by a regular diet, and THC (3 mg·kg<sup>-1</sup>) or vehicle (Veh) was administered for five consecutive days and a battery of behavioural tests was performed at 5 and 15 days of recovery. Some control animals were fed with regular diet (R.D.) or cuprizone 6 weeks (6w Cpz). (a) Animals were trained to perform the rotarod test the first week after weaning and re-evaluated during remyelination. Bar graph shows the mean latency to fall (s) at Day 5 or 15 during remyelination. (b) Beam walk test quantified as the mean time spent to cross the beam. (c) Representative images of trajectories in the open-field test, representation of total distance and the number of entries in the centre of the arena. Data are shown as mean  $\pm$  SEM;  $n = 10$  for R.D. and 6w Cpz,  $n = 8$  for d5 and d15 (a);  $n = 15$  for R.D.,  $n = 12$  for 6w Cpz,  $n = 16$  for Veh,  $n = 18$  for THC (d5),  $n = 9$  for d15 (b);  $n = 9$  for R.D., 6w Cpz and d15,  $n = 15$  for Veh,  $n = 14$  for THC (d5) (c, upper panel),  $n = 11$  for R.D.,  $n = 10$  for 6w Cpz,  $n = 15$  for Veh,  $n = 14$  for THC (d5),  $n = 8$  for d15 (c, lower panel). \* $P = 0.05$  versus vehicle-treated group; # $P = 0.05$  versus R.D., by one-way ANOVA, with uncorrected Fisher's LSD (a, c upper panel), Kruskal–Wallis one-way ANOVA with uncorrected Dunn's post hoc test (b,c lower panel)

and differentiation, we performed several cell-tracking approaches. First, we used the NG2 (neural/glial antigen 2)-Cre: Ai6 mouse line, in which tamoxifen-driven recombination induces Zs<sup>green</sup> expression in oligodendrocyte precursor cells, thus allowing cell tracking along with lineage progression during the remyelination phase. Adult NG2-Cre: Ai6 mice were fed with Cpz diet and tamoxifen was administered, followed by THC or Veh (Figure 3d). Oligodendrocyte regeneration was analysed by immunofluorescence in the corpus callosum during remyelination. Preliminary results showed an increased percentage of oligodendrocyte progenitor cell-derived Ai6<sup>+</sup> cells that co-expressed the differentiated oligodendrocyte marker CC1 during the recovery phase in the corpus callosum of THC treated-mice as compared with the Veh-treated group (Figure 3d). We also found an increased percentage of mature myelinating GST $\pi$ <sup>+</sup> cells among the recombinant Ai6<sup>+</sup> oligodendrocyte population in the corpus callosum of THC-treated mice (Figure 3d). THC-induced oligodendrocyte progenitor cell differentiation was confirmed by using the NG2-dsRed oligodendrocyte progenitor cell reporter mouse line (Zhu et al., 2008), in which the fluorescent red protein is expressed under the control of the NG2 gene promoter, thus allowing to conduct a high-resolution characterization of NG2 expression and to track its downregulation

during cell differentiation. We found a reduced percentage of NG2-dsRed<sup>+</sup> oligodendrocyte precursor cells within the Olig2<sup>+</sup> population in the corpus callosum of THC-treated mice during the recovery phase as compared with controls (Figure 3e).

We aimed to expand the aforementioned observations by performing cell cycle exit experiments based on the administration of BrdU after the Cpz diet, followed by THC or Veh injection. Immunofluorescence analysis and quantification of cycling Ki67<sup>+</sup> cells within the labelled BrdU<sup>+</sup>Olig2<sup>+</sup> population revealed a THC-evoked reduction of proliferating oligodendroglial cells (Figure 3f). Collectively, these data show that THC administration following demyelination induces oligodendrocyte progenitor cell cycle exit and differentiation, thereby enhancing oligodendrocyte regeneration and functional CNS remyelination.

### 3.4 | CB<sub>1</sub> receptor blockade prevents the THC-enhanced functional CNS remyelination

To identify the primary target of THC-induced oligodendrocyte regeneration and CNS remyelination, we co-injected NG2-dsRed mice with



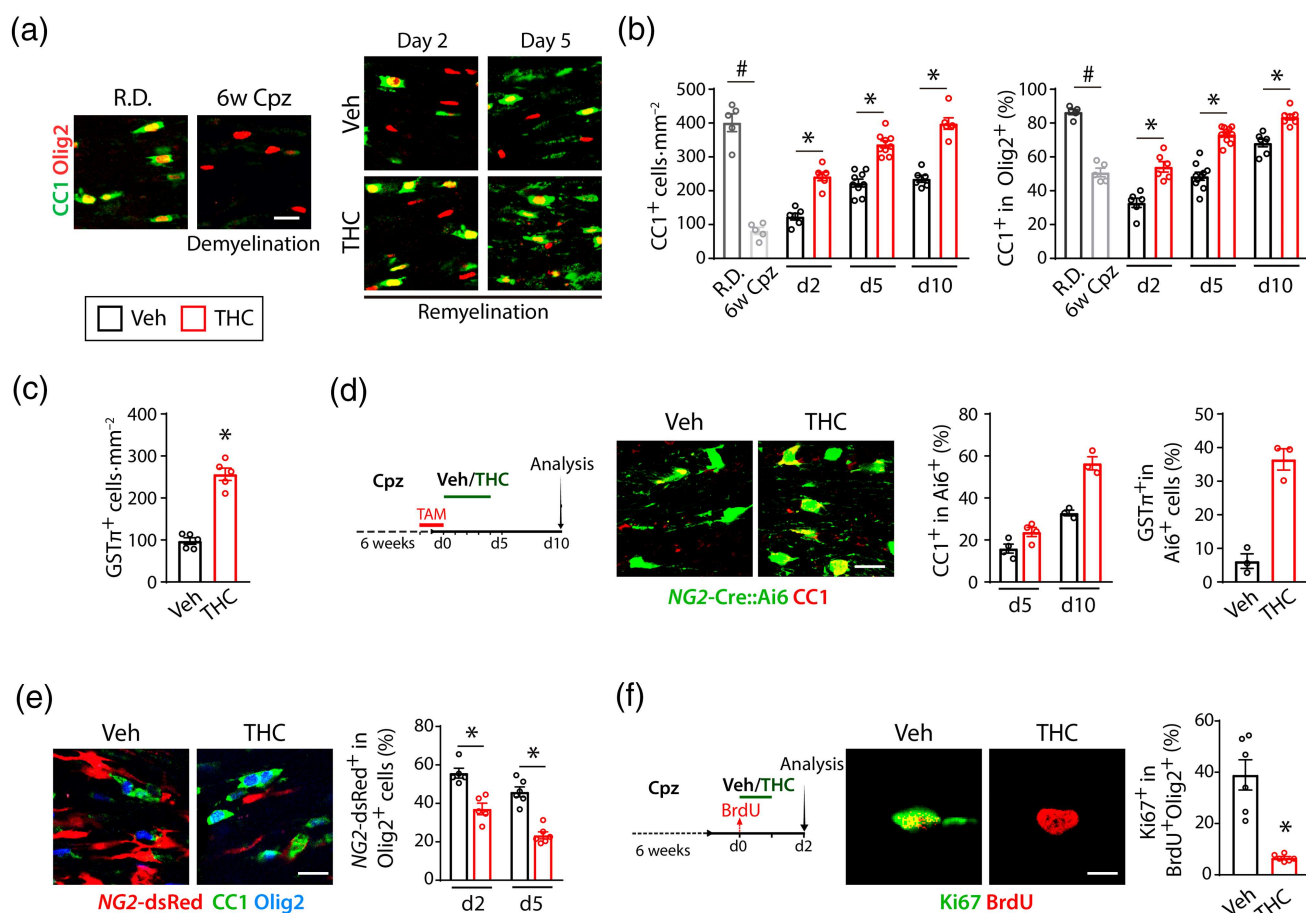
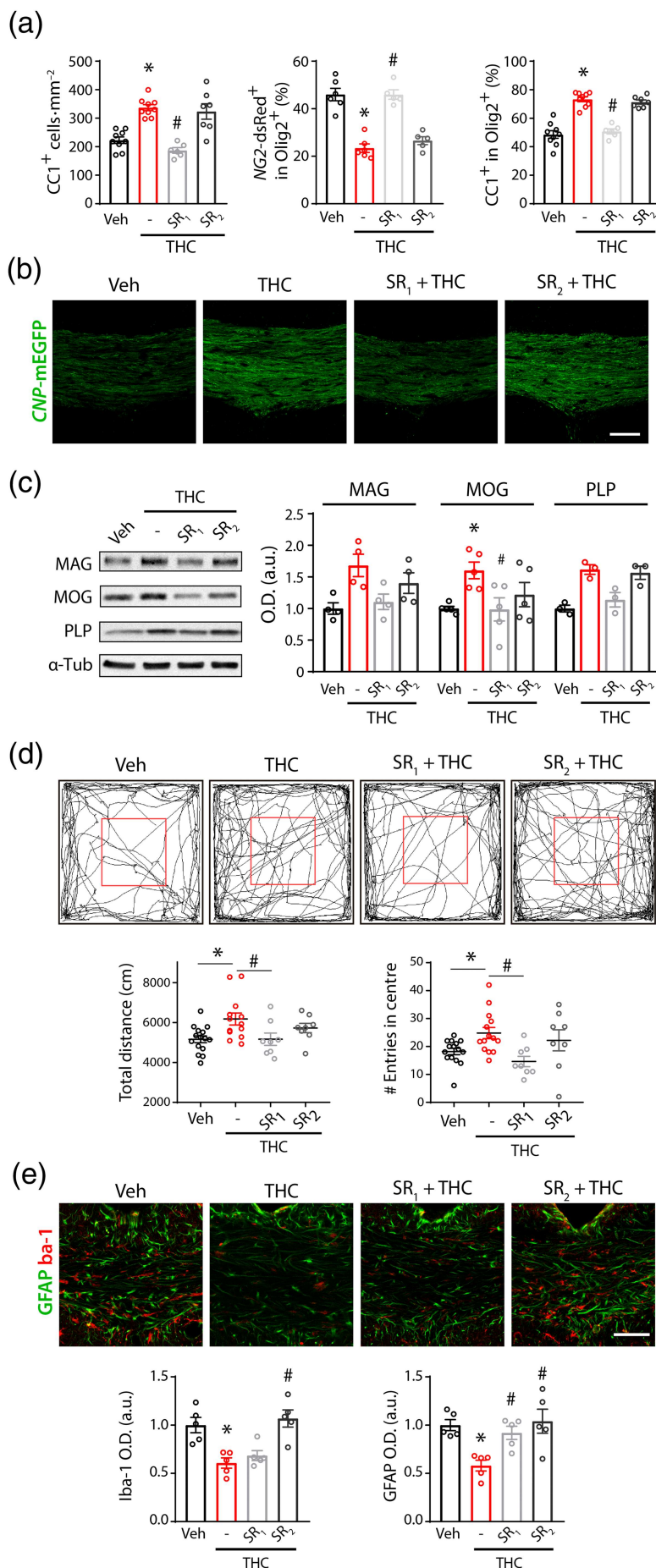


**FIGURE 3**  $\Delta^9$ -Tetrahydrocannabinol (THC) enhances oligodendrocyte regeneration during remyelination. Mice were fed with a 0.2% cuprizone (Cpz) diet for 6 weeks, followed by a regular diet, and tetrahydrocannabinol (THC) (3 mg·kg<sup>-1</sup>) or vehicle (Veh) was administered for two or five consecutive days. Oligodendrocyte regeneration was analysed by immunofluorescence analysis in the corpus callosum (CC) 2, 5 or 10 days later. Some control animals were fed with regular diet (R.D.) or cuprizone for 6 weeks (6w Cpz). (a) Representative images of anti-adenomatous polyposis coli (CC1) and oligodendrocyte transcription factor 2 (Olig2) staining in the CC. (b) Quantification of CC1<sup>+</sup> oligodendrocyte cell densities and the percentage of CC1<sup>+</sup> oligodendrocytes among Olig2<sup>+</sup> cells at Days 2, 5 and 10 of recovery. (c) Quantification of glutathione-S-transferase (GSTπ<sup>+</sup>) mature oligodendrocyte cell densities at Day 10 of recovery. (d) NG2-Cre::Ai6 mice were administered with *tamoxifen* starting 1 day before Cpz removal (three times, 24 h apart). THC or Veh administration was initiated the day following Cpz withdrawal and was given for five consecutive days. Representative confocal images and quantification of the percentage of CC1<sup>+</sup> oligodendrocytes among the recombinant Ai6<sup>+</sup> population or the percentage of GSTπ<sup>+</sup> mature oligodendrocytes among the Ai6<sup>+</sup> cells at Day 10 of recovery. (e) NG2-dsRed received THC or Veh administrations the day following Cpz withdrawal and was given for five consecutive days. Immunofluorescence analysis and quantification of the percentage of NG2-dsRed<sup>+</sup> among Olig2<sup>+</sup> cells. (f) Wild-type mice received BrdU injections the day following Cpz removal. Representative confocal images and quantification of the percentage of Ki67<sup>+</sup> cells among BrdU<sup>+</sup>Olig2<sup>+</sup> cells. Data are shown as mean ± SEM; *n* = 5 for R.D. and 6w Cpz, *n* = 6 for d2 and d10 and *n* = 9 for d5 (b); *n* = 5 (c); *n* = 4 for d2 and *n* = 3 for d10 (d); *n* = 5 for d2 and *n* = 6 for d5 (e); *n* = 6 (f). \**P* < 0.05 versus vehicle-treated group, or #*P* < 0.05 versus R.D. group by one-way ANOVA with Tukey's post hoc test (b,e), by unpaired Student's *t*-test (c) or unpaired Student's *t*-tests with Welch correction (f). Scale bars (a, d & e) = 18 μm, (f) = 8 μm

THC and the cannabinoid CB<sub>1</sub> receptor-selective antagonist rimonabant (2 mg·kg<sup>-1</sup>) or the cannabinoid CB<sub>2</sub> receptor-selective antagonist SR144528 (2 mg·kg<sup>-1</sup>). Immunofluorescence analysis of oligodendrocyte markers in corpus callosum sections revealed that the CB<sub>1</sub> receptor antagonist prevented the THC-enhanced oligodendrocyte differentiation, as revealed by quantification of CC1<sup>+</sup> cell density and NG2-dsRed or CC1 co-expression in the Olig2<sup>+</sup> population (Figure 4a). In contrast, the CB<sub>2</sub> receptor antagonist failed to prevent THC-induced oligodendrocyte regeneration. Comparable data

were obtained in the CNP-mEGFP reporter mouse line, in which CB<sub>1</sub> receptor blockade prevented the THC-induced increase of CNP-mEGFP reactivity in the corpus callosum during the remyelination phase (Figure 4b). Likewise, exploratory western blot analysis of corpus callosum extracts obtained at the recovery phase showed that pharmacological blockade of the CB<sub>1</sub> receptor, but not CB<sub>2</sub> receptor prevented the THC-induced increase of myelin proteins in the corpus callosum (Figure 4c). Furthermore, the analysis of behavioural parameters showed that CB<sub>1</sub> receptor blockade prevented the THC-evoked

**FIGURE 4** CB<sub>1</sub> receptors antagonism prevents the  $\Delta^9$ -tetrahydrocannabinol (THC)-enhanced oligodendrocyte regeneration and functional remyelination. Wild-type c57/BL6 (c, d, & e), NG2-dsRed (a) or CNP-mEGFP (b) mice were fed with a 0.2% cuprizone (Cpz) diet for 6 weeks, followed by a regular diet. At 24 h, after cuprizone removal, rimonabant (SR<sub>1</sub>, 2 mg·kg<sup>-1</sup>) or SR-144528 (SR<sub>2</sub>; 2 mg·kg<sup>-1</sup>), selective CB<sub>1</sub> or CB<sub>2</sub> respective cannabinoid receptors antagonists, were administered 30 min before THC (3 mg·kg<sup>-1</sup>) for five consecutive days and oligodendrocyte regeneration, and CNS remyelination was analysed in the corpus callosum (CC) 5 days after the first THC administration. (a) Quantification of APC, anti-adenomatous polyposis coli (CC1)<sup>+</sup>, oligodendrocyte cell density and the percentage of NG2-dsRed<sup>+</sup> oligodendrocyte progenitor cell or CC1<sup>+</sup> cells among Olig2<sup>+</sup> cells. (b) Representative confocal images of the CC of CNP-mEGFP mice at Day 5 of recovery. (c) Representative scans and optical density (O.D.) values of western blot analysis of myelin-associated protein levels of dissected CC extracts at Day 5 of recovery. O.D. values are relative to those of their respective loading controls and expressed as arbitrary units (a.u.). Myelin-associated glycoprotein (MAG), myelin oligodendrocyte glycoprotein (MOG) and proteolipid protein (PLP). (d) Representative images of trajectories in the open-field test, quantification of total distance and the number of entries in the centre of the arena. (e) Representative confocal images and quantification of microglial (Iba1) and astroglial (GFAP) markers. Data are shown as mean  $\pm$  SEM;  $n = 9$  for Veh and THC,  $n = 6$  for SR<sub>1</sub>,  $n = 7$  for SR<sub>2</sub> (a, left and right panels),  $n = 6$  for Veh and THC,  $n = 5$  for SR<sub>1</sub> and SR<sub>2</sub> (a, middle panel);  $n = 5$  (b),  $n = 4$  for MAG,  $n = 5$  for MOG,  $n = 3$  for PLP (c);  $n = 15$  for Veh,  $n = 14$  for THC,  $n = 8$  for SR<sub>1</sub> and SR<sub>2</sub> (d);  $n = 5$  (e). \* $P < 0.05$  versus vehicle-treated group or # $P < 0.05$  versus THC, by one-way ANOVA with Tukey's post hoc test (a, c, & e), and with uncorrected Fisher's LSD (d). Scale bars (b,e) = 60  $\mu$ m



motor function recovery during remyelination, as analysed in the open-field test (Figure 4d).

Cannabinoid compounds have been shown to exert prominent anti-neuroinflammatory actions in multiple sclerosis experimental models (Al-Ghezi et al., 2019; Gonzalez-Garcia et al., 2017; Lyman et al., 1989; Wirguin et al., 1994). Immunofluorescence analysis in the

corpus callosum revealed a reduced immunoreactivity of ionized calcium-binding adapter molecule 1 (IBA1) and glial fibrillary acidic protein (GFAP) in THC-treated mice compared with Veh-treated animals (Figure 4e). In addition, administration of either rimonabant or SR144528 prevented the THC-induced attenuation of astroglial activation during remyelination, whereas microglial activation was

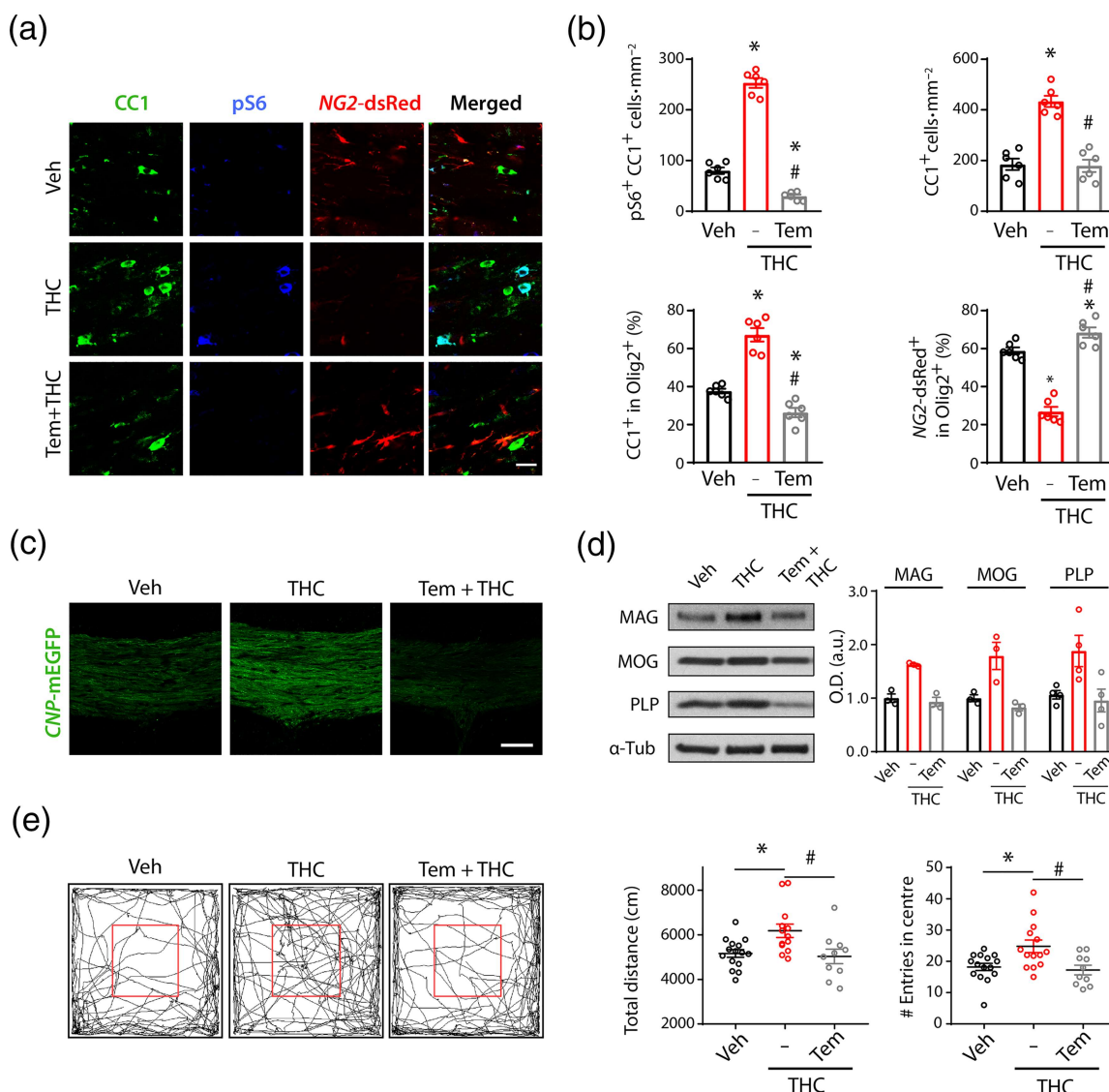


**FIGURE 5** mTORC<sub>1</sub> blockade prevents the  $\Delta^9$ -tetrahydrocannabinol (THC)-enhanced oligodendrocyte regeneration and functional remyelination. Adult NG2-dsRed or CNP-mEGFP mice were fed with a 0.2% cuprizone (Cpz) diet for 6 weeks, followed by regular diet. At 24 h, after cuprizone removal, the mTORC<sub>1</sub> selective inhibitor temsirolimus (Tem; 5 mg·kg<sup>-1</sup>), was administered at 30 min before THC (3 mg·kg<sup>-1</sup>) for five consecutive days, and oligodendrocyte regeneration and remyelination was analysed in corpus callosum (CC) 5 days after the first THC administration. (a,b) Immunofluorescence analysis of mTORC<sub>1</sub> activation levels in oligodendroglial cells. Confocal representative images and quantification of pS6<sup>+</sup> anti-adenomatous polyposis coli (CC1<sup>+</sup>) and CC1<sup>+</sup> oligodendrocyte cell densities, the percentage of NG2-dsRed<sup>+</sup> or CC1<sup>+</sup> cells among Olig2<sup>+</sup> cells. S6, ribosomal protein; CC1, APC, anti-adenomatous polyposis coli. (c) Representative confocal images of the CC of CNP-mEGFP mice at Day 5 of recovery. (d) Representative scans and optical density (O.D.) values of western blot analysis of myelin-associated protein levels of CC extracts at Day 5 of recovery. O.D. values are relative to those of their respective loading controls and expressed as arbitrary units (a.u.). Myelin-associated glycoprotein (MAG), myelin oligodendrocyte glycoprotein (MOG) and proteolipid protein (PLP). (e) Representative images of trajectories in the open-field test. Graph representation of total distance travelled and the number of entries in the centre of the arena at Day 5 of recovery. Data are shown as mean  $\pm$  SEM:  $n = 6$  (b);  $n = 5$  (c);  $n = 3$  for MAG and MOG,  $n = 4$  for PLP (d);  $n = 15$  for Veh,  $n = 14$  for THC,  $n = 10$  for Tem (e). \* $P < 0.05$  versus vehicle-treated group or # $P < 0.05$  versus THC-treated group, by one-way ANOVA with Tukey's post hoc test (b,d), and with uncorrected Fisher's LSD (e). Scale bars (a) = 18  $\mu$ m; (c) = 60  $\mu$ m



only prevented by SR144528 (Figure 4e). These data indicate that THC attenuates glial activation during remyelination via CB<sub>1</sub> and CB<sub>2</sub> receptor activation.

### 3.5 | mTORC<sub>1</sub> blockade prevents the THC-enhanced functional CNS remyelination

Mammalian target of rapamycin complex 1 (mTORC<sub>1</sub>) is an essential modulator of oligodendrocyte differentiation during CNS myelination and remyelination (Gaesser & Fyffe-Maricich, 2016; Ishii et al., 2019; McLane et al., 2017; Wood et al., 2013). Thus, mTORC<sub>1</sub> signalling blockade has been shown to abolish spontaneous remyelination following Cpz-induced demyelination (Bai et al., 2016; Sachs et al., 2014). Moreover, CB<sub>1</sub> receptors have been shown to regulate this signalling pathway during oligodendrocyte development (Gomez et al., 2015; Hueriga-Gomez et al., 2020). Therefore, we explored the involvement of the mTORC<sub>1</sub> signalling pathway in the observed THC effects during remyelination. We found increased phosphorylation levels of the mTORC<sub>1</sub> axis-readout protein S6 in CC1<sup>+</sup> oligodendrocytes in the corpus callosum of THC-treated mice during remyelination (Figure 5a,b), as compared with the control group.

To evaluate the contribution of oligodendrocyte regeneration in the THC-enhanced functional remyelination, we administered the mTORC<sub>1</sub> inhibitor temsirolimus together with THC, for five consecutive days, and oligodendrogenesis was analysed during the recovery phase. mTORC<sub>1</sub> pharmacological blockade prevented the THC-induced increase of CC1<sup>+</sup> and pS6<sup>+</sup>CC1<sup>+</sup> cell densities, CC1 co-expression in the Olig2<sup>+</sup> population and the THC-evoked reduction of the percentage of Olig2<sup>+</sup> cells that expressed NG2-dsRed (Figure 5a,b). Temsirolimus also prevented the THC-induced oligodendrocyte regeneration in the corpus callosum, when quantifying CNP-mEGFP reactivity in tissue sections (Figure 5c), and corpus callosum remyelination, when quantifying myelin-associated protein levels in exploratory western blot analysis of corpus callosum extracts (Figure 5d). The analysis of behavioural parameters showed that mTORC<sub>1</sub> pharmacological blockade also abolished the THC-enhanced motor function recovery during remyelination in the open-field test (Figure 5e). Altogether, these findings suggest that THC administration following demyelination induces functional oligodendrocyte regeneration and CNS remyelination, at least in part by activating the mTORC<sub>1</sub> signalling pathway in cells of the oligodendrocyte lineage. Moreover, our study indicates that the observed THC-enhanced functional recovery comes at the expense of enhanced oligodendrocyte regeneration.

## 4 | DISCUSSION AND CONCLUSIONS

Accruing evidence supports a neuroprotective and immunomodulatory action of THC in multiple sclerosis animal models (Pryce et al., 2015). Here, we identify CNS remyelination as a key mechanism underlying THC protective actions under demyelinating conditions.

THC-induced functional recovery in multiple sclerosis animal models may be therefore mediated, at least in part, by oligodendrocyte regeneration and CNS remyelination. To date, most of the preclinical studies of THC in multiple sclerosis have shown potent immunosuppressive actions, which modulate disease progression and ameliorate disability in immune-mediated animal models of demyelination (Gonzalez-Garcia et al., 2017; Lyman et al., 1989; Pryce et al., 2003). These studies have shown that THC administration slows down inflammation-mediated disability during relapsing disease in mice, at least in part by attenuating immune cell infiltration into the CNS. However, although non-sedating doses of THC do not inhibit relapsing autoimmunity in the experimental autoimmune encephalomyelitis model, they dose-dependently inhibit the accumulation of disability (Croxford et al., 2008; Pryce et al., 2015), suggesting a regenerative action of THC in this animal model. The complex immunomodulatory actions of THC in immune-mediated demyelination animal models can therefore mask the regenerative capacity of the compound.

To study the regenerative capacity of THC administration, and trying to minimize the potential immunomodulatory actions reported in immune-mediated demyelination animal models, here, we used a well-established toxin animal model of demyelination, with more discrete phases of demyelination and remyelination, and in which immune cell activity during the remyelination phase is more likely a response to myelin damage rather than the cause of the demyelination process (Hooijmans et al., 2019; McMurrin et al., 2016). Acute THC administration following Cpz-induced demyelination enhances oligodendrocyte progenitor cell cycle exit and differentiation, thus suggesting that it may act cell-autonomously by activating CB<sub>1</sub> receptors in oligodendrocyte precursor cells, thereby promoting cell differentiation and oligodendrocyte regeneration. As CB<sub>1</sub> receptors are abundantly expressed in various neuronal and glial cell populations (Di Marzo et al., 2015), we cannot exclude the possibility that CB<sub>1</sub> receptor modulation of oligodendrocyte progenitor cell differentiation involves other non-oligodendrocyte progenitor cell populations. First, CB<sub>1</sub> receptor-mediated neuroprotection may favour neuronal integrity and functionality, thereby impacting the process of oligodendrocyte regeneration and efficient remyelination (Gautier et al., 2015; Spitzer et al., 2016). A CB<sub>1</sub> receptor-restored glutamate neurotransmission may positively influence oligodendrocyte regeneration and CNS remyelination (Gautier et al., 2015; Spitzer et al., 2016). Moreover, a more neuroprotective environment would also conceivably reduce toxicity and neuroinflammation, and in turn, facilitate remyelination (Franklin & Ffrench-Constant, 2017). Second, the observed effect of THC in attenuating glial activation may also favour an efficient environment for brain regenerative capacity (Lloyd et al., 2017; Molina-Gonzalez & Miron, 2019). Third, THC could modulate as well peripheral immune activation and indirectly impact the neuroinflammatory status (Bouchard et al., 2012; Rizzo et al., 2020). Indeed, in the Cpz model, blood brain barrier integrity is compromised even before the demyelination process occurs (Berghoff, Duking, et al., 2017; Berghoff, Gerndt, et al., 2017; Shelestak et al., 2020), thereby allowing immune cell infiltration and impacting the process of oligodendrocyte regeneration and efficient remyelination (Lloyd



et al., 2017; McMurran et al., 2016; Molina-Gonzalez & Miron, 2019). This possibility seems, however, unlikely if we consider that the low THC dose tested in this study seems to be devoid of immunomodulatory activity at the peripheral level (Croxford et al., 2008). Thus, elucidating the precise cellular targets of THC-enhanced remyelination requires further studies.

Oligodendrocyte precursor cells express CB<sub>1</sub> and CB<sub>2</sub> receptors at developmental stages and respond to selective pharmacological modulation by synthetic or endogenous cannabinoids (Arevalo-Martin et al., 2007; Gomez et al., 2015; Huerga-Gomez et al., 2020; Molina-Holgado et al., 2002; Moreno-Luna et al., 2020). In addition, THC has been shown to modulate oligodendrogenesis during postnatal myelination through CB<sub>1</sub> and CB<sub>2</sub> receptor activation (Huerga-Gomez et al., 2020). In the present study, we have found that CB<sub>1</sub> receptor-mediated induction of oligodendrocyte regeneration and CNS remyelination is indeed effective under demyelinating conditions in adult mice. However, CB<sub>2</sub> receptor antagonism does not prevent the regenerative capacity of THC, while efficiently preventing the THC-mediated attenuation of glial activation. Similarly, CB<sub>1</sub> receptors have been pointed out as the main mediators of the Sativex-induced disease-modifying effects in the experimental autoimmune encephalomyelitis and Theiler's murine encephalomyelitis virus (TMEV) animal models (Feliu et al., 2015; Moreno-Martet et al., 2015). Thus, the specific contribution of both receptors in the disease-modifying actions of THC in multiple sclerosis animal models remain to be firmly established.

Moreover, the most common plant-derived pharmaceutical-grade preparations or cannabis extracts used in the treatment of multiple sclerosis patients contain THC together with CBD (Messina et al., 2017; Russo, 2011). CBD has been shown to slow down inflammation-mediated disability during relapsing disease in experimental autoimmune encephalomyelitis mice, at least in part by attenuating immune cell infiltration into the CNS (Gonzalez-Garcia et al., 2017), inducing myeloid-derived suppressor cells (Elliott et al., 2018), and attenuating neuronal apoptosis (Giacoppo et al., 2015). CBD also prevents hypoxia/ischemia-induced hypomyelination in newborn rats (Ceprian et al., 2019), suggesting that it could potentially modulate CNS remyelination in multiple sclerosis animal models. Thus, THC and CBD could synergistically modulate remyelination and functional recovery in multiple sclerosis animal models. Indeed, CBD has been shown to synergize with THC-improved motor function in the TMEV model of demyelination (Feliu et al., 2015). Thus, the potential interaction of the two main phytocannabinoids in modulating remyelination in multiple sclerosis animal models still need to be determined.

Our study provides a novel therapeutic advantage of THC-based interventions in multiple sclerosis by promoting remyelination and functional recovery. New clinical trials with improved designs on cannabinoids in people with multiple sclerosis are needed now, considering these compounds as potential remyelinating/disease-modifying drugs to try to overcome previous failures (Zajicek et al., 2013). Our work also suggests that at least part of the neuroprotective action of phytocannabinoids in multiple sclerosis

animal models and potentially in patients as well may be due to an enhanced CNS remyelination. Finally, this study also identifies THC as a potent inducer of oligodendrocyte progenitor cell differentiation under demyelination in mice, opening the possibility for this molecule to become a candidate drug to promote oligodendrocyte regeneration and remyelination in the treatment of demyelinating disorders.

## ACKNOWLEDGEMENTS

This work was supported by the MINECO Grants SAF2017-83516 and PID2020-112640RB-I00, and the Comunidad de Madrid Grants 2016-T1/BMD-1060 and 2020-5A/BMD-19728, Atracción del Talento Investigador Program, to J.P., A.H.G. and T.A. were supported by 2016-T1/BMD-1060 and Comunidad de Madrid contract, and A.S. T by Fundación Tatiana Pérez de Guzmán el Bueno. Support was also provided by MINECO (Grants RTI2018-095311-B-I00 to M.G. and SAF2016-75292-R to C.M.), CIBERNED (Grants CB06/05/0005 to M.G. and CB06/0005/0076 to C.M.), FEDER and ISCIII (AES 2018 Grants PI18-00941 to I.G.-R. and PI18/00513 to S.M.), Basque Government (Eusko Jaurlaritz, Grants IT1203-19 to C.M. and PIBA19-0059 to S.M.) and ARSEP Foundation (Grant to S.M.). We are indebted to NIH for donating the rimonabant and the SR144528.

## AUTHOR CONTRIBUTIONS

TA and JP designed research, analysed data and wrote the manuscript. TA, AH, AST, ER and JCC performed research. MG, IGR, SM and CM contributed to write the manuscript. All authors read and approved the final manuscript.

## CONFLICT OF INTERESTS

The authors declare that they have no competing interest.

## DECLARATION OF TRANSPARENCY AND SCIENTIFIC RIGOUR

This Declaration acknowledges that this paper adheres to the principles for transparent reporting and scientific rigour of preclinical research as stated in the BJP guidelines for [Design and Analysis](#), [Immunoblotting and Immunochemistry](#) and [Animal Experimentation](#), and as recommended by funding agencies, publishers and other organizations engaged with supporting research.

## DATA AVAILABILITY STATEMENT

All data generated or analysed during this study are available from the corresponding author on reasonable request.

## ORCID

Tania Aguado  <https://orcid.org/0000-0003-4339-0443>

Ismael Galve-Roperh  <https://orcid.org/0000-0003-3501-2434>

Javier Palazuelos  <https://orcid.org/0000-0002-0409-1398>

## REFERENCES

Alexander, S. P. H., Christopoulos, A., Davenport, A. P., Kelly, E., Mathie, A., Peters, J. A., Veale, E. L., Armstrong, J. F., Faccenda, E.,

- Harding, S. D., Pawson, A. J., Sharman, J. L., Southan, C., Davies, J. A., & CGTP Collaborators. (2019). The Concise Guide to PHARMACOLOGY 2019/20: G protein-coupled receptors. *British Journal of Pharmacology*, 176(Suppl 1), S21–S141. <https://doi.org/10.1111/bph.14748>
- Alexander, S. P. H., Roberts, R. E., Broughton, B. R. S., Sobey, C. G., George, C. H., Stanford, S. C., Cirino, G., Docherty, J. R., Giembycz, M. A., Hoyer, D., Insel, P. A., Izzo, A. A., Ji, Y., MacEwan, D. J., Mangum, J., Wonnacott, S., & Ahluwalia, A. (2018). Goals and practicalities of immunoblotting and immunohistochemistry: A guide for submission to the British Journal of Pharmacology. *British Journal of Pharmacology*, 175(3), 407–411. <https://doi.org/10.1111/bph.14112>
- Al-Ghezi, Z. Z., Busbee, P. B., Alghetaa, H., Nagarkatti, P. S., & Nagarkatti, M. (2019). Combination of cannabinoids, delta-9-tetrahydrocannabinol (THC) and cannabidiol (CBD), mitigates experimental autoimmune encephalomyelitis (EAE) by altering the gut microbiome. *Brain, Behavior, and Immunity*, 82, 25–35. <https://doi.org/10.1016/j.bbi.2019.07.028>
- Arevalo-Martin, A., Garcia-Ovejero, D., Rubio-Araiz, A., Gomez, O., Molina-Holgado, F., & Molina-Holgado, E. (2007). Cannabinoids modulate Olig2 and polysialylated neural cell adhesion molecule expression in the subventricular zone of post-natal rats through cannabinoid receptor 1 and cannabinoid receptor 2. *The European Journal of Neuroscience*, 26(6), 1548–1559. <https://doi.org/10.1111/j.1460-9568.2007.05782.x>
- Bai, C. B., Sun, S., Roholt, A., Benson, E., Edberg, D., Medicetty, S., Dutta, R., Kidd, G., Macklin, W. B., & Trapp, B. (2016). A mouse model for testing remyelinating therapies. *Experimental Neurology*, 283(Pt A), 330–340. <https://doi.org/10.1016/j.expneurol.2016.06.033>
- Berghoff, S. A., Dusing, T., Spieth, L., Winchenbach, J., Stumpf, S. K., Gerndt, N., Kusch, K., Ruhwedel, T., Möbius, W., & Saher, G. (2017). Blood-brain barrier hyperpermeability precedes demyelination in the cuprizone model. *Acta Neuropathologica Communications*, 5(1), 94. <https://doi.org/10.1186/s40478-017-0497-6>
- Berghoff, S. A., Gerndt, N., Winchenbach, J., Stumpf, S. K., Hosang, L., Odoardi, F., Ruhwedel, T., Böhrer, C., Barrette, B., Stassart, R., Liebetanz, D., Dibaj, P., Möbius, W., Edgar, J. M., & Saher, G. (2017). Dietary cholesterol promotes repair of demyelinated lesions in the adult brain. *Nature Communications*, 8, 14241. <https://doi.org/10.1038/ncomms14241>
- Bernal-Chico, A., Canedo, M., Manterola, A., Victoria Sanchez-Gomez, M., Perez-Samartin, A., Rodriguez-Puertas, R., Matute, C., & Mato, S. (2015). Blockade of monoacylglycerol lipase inhibits oligodendrocyte excitotoxicity and prevents demyelination in vivo. *Glia*, 63(1), 163–176. <https://doi.org/10.1002/glia.22742>
- Bolcskei, K., Kriszta, G., Saghy, E., Payrits, M., Sipos, E., Vranesics, A., Berente, Z., Ábrahám, H., Ács, P., Komoly, S., & Pinter, E. (2018). Behavioural alterations and morphological changes are attenuated by the lack of TRPA1 receptors in the cuprizone-induced demyelination model in mice. *Journal of Neuroimmunology*, 320, 1–10. <https://doi.org/10.1016/j.jneuroim.2018.03.020>
- Bouchard, J., Truong, J., Bouchard, K., Dunkelberger, D., Desrayaud, S., Moussaoui, S., Tabrizi, S. J., Stella, N., & Muchowski, P. J. (2012). Cannabinoid receptor 2 signaling in peripheral immune cells modulates disease onset and severity in mouse models of Huntington's disease. *The Journal of Neuroscience*, 32(50), 18259–18268. <https://doi.org/10.1523/JNEUROSCI.4008-12.2012>
- Ceprian, M., Vargas, C., Garcia-Toscano, L., Penna, F., Jimenez-Sanchez, L., Achicallende, S., Elezgarai, I., Grandes, P., Hind, W., Pazos, M. R., & Martinez-Orgado, J. (2019). Cannabidiol administration prevents hypoxia-ischemia-induced hypomyelination in newborn rats. *Frontiers in Pharmacology*, 10, 1131. <https://doi.org/10.3389/fphar.2019.01131>
- Chari, D. M. (2007). Remyelination in multiple sclerosis. *International Review of Neurobiology*, 79, 589–620. [https://doi.org/10.1016/S0074-7742\(07\)79026-8](https://doi.org/10.1016/S0074-7742(07)79026-8)
- Cofield, S. S., Salter, A., Tyry, T., Crowe, C., Cutter, G. R., Fox, R. J., & Marrie, R. A. (2017). Perspectives on marijuana use and effectiveness: A survey of NARCOMS participants. *Neurology: Clinical Practice*, 7(4), 333–343. <https://doi.org/10.1212/CPJ.0000000000000383>
- Croxford, J. L., Pryce, G., Jackson, S. J., Ledent, C., Giovannoni, G., Pertwee, R. G., Yamamura, T., & Baker, D. (2008). Cannabinoid-mediated neuroprotection, not immunosuppression, may be more relevant to multiple sclerosis. *Journal of Neuroimmunology*, 193(1–2), 120–129. <https://doi.org/10.1016/j.jneuroim.2007.10.024>
- Cuniffe, N., & Coles, A. (2019). Promoting remyelination in multiple sclerosis. *Journal of Neurology*, 268, 30–44. <https://doi.org/10.1007/s00415-019-09421-x>
- Curtis, M. J., Alexander, S., Cirino, G., Docherty, J. R., George, C. H., Giembycz, M. A., Hoyer, D., Insel, P. A., Izzo, A. A., Ji, Y., MacEwan, D. J., Sobey, C. G., Stanford, S. C., Teixeira, M. M., Wonnacott, S., & Ahluwalia, A. (2018). Experimental design and analysis and their reporting II: Updated and simplified guidance for authors and peer reviewers. *British Journal of Pharmacology*, 175(7), 987–993. <https://doi.org/10.1111/bph.14153>
- Deng, Y., Kim, B., He, X., Kim, S., Lu, C., Wang, H., Cho, S. G., Hou, Y., Li, J., Zhao, X., & Lu, Q. R. (2014). Direct visualization of membrane architecture of myelinating cells in transgenic mice expressing membrane-anchored EGFP. *Genesis*, 52(4), 341–349. <https://doi.org/10.1002/dvg.22751>
- Di Marzo, V., Stella, N., & Zimmer, A. (2015). Endocannabinoid signalling and the deteriorating brain. *Nature Reviews. Neuroscience*, 16(1), 30–42. <https://doi.org/10.1038/nrn3876>
- Dubois-Dalq, M., Williams, A., Stadelmann, C., Stankoff, B., Zalc, B., & Lubetzki, C. (2008). From fish to man: Understanding endogenous remyelination in central nervous system demyelinating diseases. *Brain*, 131(Pt 7), 1686–1700. <https://doi.org/10.1093/brain/awn076>
- Duncan, I. D., Brower, A., Kondo, Y., Curlee, J. F. Jr., & Schultz, R. D. (2009). Extensive remyelination of the CNS leads to functional recovery. *Proceedings of the National Academy of Sciences of the United States of America*, 106(16), 6832–6836. <https://doi.org/10.1073/pnas.0812500106>
- Eljaschewitsch, E., Witting, A., Mawrin, C., Lee, T., Schmidt, P. M., Wolf, S., Hoertnagl, H., Raine, C. S., Schneider-Stock, R., Nitsch, R., & Ullrich, O. (2006). The endocannabinoid anandamide protects neurons during CNS inflammation by induction of MKP-1 in microglial cells. *Neuron*, 49(1), 67–79. <https://doi.org/10.1016/j.neuron.2005.11.027>
- Elliott, D. M., Singh, N., Nagarkatti, M., & Nagarkatti, P. S. (2018). Cannabidiol attenuates experimental autoimmune encephalomyelitis model of multiple sclerosis through induction of myeloid-derived suppressor cells. *Frontiers in Immunology*, 9, 1782. <https://doi.org/10.3389/fimmu.2018.01782>
- Feliu, A., Moreno-Martet, M., Mecha, M., Carrillo-Salinas, F. J., de Lago, E., Fernandez-Ruiz, J., & Guaza, C. (2015). A Sativex([R])-like combination of phytocannabinoids as a disease-modifying therapy in a viral model of multiple sclerosis. *British Journal of Pharmacology*, 172(14), 3579–3595. <https://doi.org/10.1111/bph.13159>
- Franco-Pons, N., Torrente, M., Colomina, M. T., & Vilella, E. (2007). Behavioral deficits in the cuprizone-induced murine model of demyelination/remyelination. *Toxicology Letters*, 169(3), 205–213. <https://doi.org/10.1016/j.toxlet.2007.01.010>
- Franklin, R. J., & Ffrench-Constant, C. (2008). Remyelination in the CNS: From biology to therapy. *Nature Reviews. Neuroscience*, 9(11), 839–855. <https://doi.org/10.1038/nrn2480>
- Franklin, R. J. M., & Ffrench-Constant, C. (2017). Regenerating CNS myelin—From mechanisms to experimental medicines. *Nature*

- Reviews. *Neuroscience*, 18(12), 753–769. <https://doi.org/10.1038/nrn.2017.136>
- Gaesser, J. M., & Fyffe-Maricich, S. L. (2016). Intracellular signaling pathway regulation of myelination and remyelination in the CNS. *Experimental Neurology*, 283(Pt B), 501–511. <https://doi.org/10.1016/j.expneurol.2016.03.008>
- Gallo, V., & Armstrong, R. C. (2008). Myelin repair strategies: A cellular view. *Current Opinion in Neurology*, 21(3), 278–283. <https://doi.org/10.1097/WCO.0b013e3282fd1875>
- Gautier, H. O., Evans, K. A., Volbracht, K., James, R., Sitnikov, S., Lundgaard, I., James, F., Lao-Peregrin, C., Reynolds, R., Franklin, R. J., & Káradóttir, R. T. (2015). Neuronal activity regulates remyelination via glutamate signalling to oligodendrocyte progenitors. *Nature Communications*, 6, 8518. <https://doi.org/10.1038/ncomms9518>
- Giaccopo, S., Soundara Rajan, T., Galuppo, M., Pollastro, F., Grassi, G., Bramanti, P., & Mazzon, E. (2015). Purified cannabidiol, the main non-psychoactive component of *Cannabis sativa*, alone, counteracts neuronal apoptosis in experimental multiple sclerosis. *European Review for Medical and Pharmacological Sciences*, 19(24), 4906–4919. Retrieved from <https://www.ncbi.nlm.nih.gov/pubmed/26744883>
- Gibson, E. M., Purger, D., Mount, C. W., Goldstein, A. K., Lin, G. L., Wood, L. S., Inema, I., Miller, S. E., Bieri, G., Zuchero, J. B., Barres, B. A., Woo, P. J., Vogel, H., & Monje, M. (2014). Neuronal activity promotes oligodendrogenesis and adaptive myelination in the mammalian brain. *Science*, 344(6183), 1252304. <https://doi.org/10.1126/science.1252304>
- Gomez, O., Sanchez-Rodriguez, M. A., Ortega-Gutierrez, S., Vazquez-Villa, H., Guaza, C., Molina-Holgado, F., & Molina-Holgado, E. (2015). A basal tone of 2-arachidonoylglycerol contributes to early oligodendrocyte progenitor proliferation by activating phosphatidylinositol 3-kinase (PI3K)/AKT and the mammalian target of rapamycin (mTOR) pathways. *Journal of Neuroimmune Pharmacology*, 10(2), 309–317. <https://doi.org/10.1007/s11481-015-9609-x>
- Gonzalez-Garcia, C., Torres, I. M., Garcia-Hernandez, R., Campos-Ruiz, L., Esparragoza, L. R., Coronado, M. J., Grande, A. G., Garcia-Merino, A., & Sanchez Lopez, A. J. (2017). Mechanisms of action of cannabidiol in adoptively transferred experimental autoimmune encephalomyelitis. *Experimental Neurology*, 298(Pt A), 57–67. <https://doi.org/10.1016/j.expneurol.2017.08.017>
- Han, S. R., Kang, Y. H., Jeon, H., Lee, S., Park, S. J., Song, D. Y., Min, S. S., Yoo, S. M., Lee, M. S., & Lee, S. H. (2020). Differential expression of miRNAs and behavioral change in the cuprizone-induced demyelination mouse model. *International Journal of Molecular Sciences*, 21(2), 646. <https://doi.org/10.3390/ijms21020646>
- Hildebrand, A., Minnier, J., & Cameron, M. H. (2020). Cannabis use for symptom relief in multiple sclerosis: A cross-sectional survey of webinar attendees in the US and Canada. *Multiple Sclerosis and Related Disorders*, 38, 101516. <https://doi.org/10.1016/j.msard.2019.101516>
- Hooijmans, C. R., Hlavica, M., Schuler, F. A. F., Good, N., Good, A., Baumgartner, L., Galeno, G., Schneider, M. P., Jung, T., de Vries, R., & Ineichen, B. V. (2019). Remyelination promoting therapies in multiple sclerosis animal models: A systematic review and meta-analysis. *Scientific Reports*, 9(1), 822. <https://doi.org/10.1038/s41598-018-35734-4>
- Huerta-Gomez, A., Aguado, T., Sanchez-de la Torre, A., Bernal-Chico, A., Matute, C., Mato, S., Guzmán, M., Galve-Roperh, I., & Palazuelos, J. (2020). Delta(9)-tetrahydrocannabinol promotes oligodendrocyte development and CNS myelination in vivo. *Glia*, 69, 532–545. <https://doi.org/10.1002/glia.23911>
- Ishii, A., Furusho, M., Macklin, W., & Bansal, R. (2019). Independent and cooperative roles of the Mek/ERK1/2-MAPK and PI3K/Akt/mTOR pathways during developmental myelination and in adulthood. *Glia*, 67(7), 1277–1295. <https://doi.org/10.1002/glia.23602>
- Lilley, E., Stanford, S. C., Kendall, D. E., Alexander, S. P., Cirino, G., Docherty, J. R., George, C. H., Insel, P. A., Izzo, A. A., Ji, Y., Panettieri, R. A., Sobey, C. G., Stefanska, B., Stephens, G., Teixeira, M., & Ahluwalia, A. (2020). ARRIVE 2.0 and the *British Journal of Pharmacology*: Updated guidance for 2020. *British Journal of Pharmacology*, 177, 3611–3616. <https://doi.org/10.1111/bph.15178>
- Lloyd, A. F., Davies, C. L., & Miron, V. E. (2017). Microglia: Origins, homeostasis, and roles in myelin repair. *Current Opinion in Neurobiology*, 47, 113–120. <https://doi.org/10.1016/j.conb.2017.10.001>
- Long, L. E., Chesworth, R., Huang, X. F., McGregor, I. S., Arnold, J. C., & Karl, T. (2010). A behavioural comparison of acute and chronic Delta9-tetrahydrocannabinol and cannabidiol in C57BL/6JArc mice. *The International Journal of Neuropsychopharmacology*, 13(7), 861–876. <https://doi.org/10.1017/S1461145709990605>
- Lyman, W. D., Sonett, J. R., Brosnan, C. F., Elkin, R., & Bornstein, M. B. (1989). Delta 9-tetrahydrocannabinol: A novel treatment for experimental autoimmune encephalomyelitis. *Journal of Neuroimmunology*, 23(1), 73–81. [https://doi.org/10.1016/0165-5728\(89\)90075-1](https://doi.org/10.1016/0165-5728(89)90075-1)
- Maccarrone, M., Maldonado, R., Casas, M., Henze, T., & Centonze, D. (2017). Cannabinoids therapeutic use: What is our current understanding following the introduction of THC, THC:CBD oromucosal spray and others? *Expert Review of Clinical Pharmacology*, 10(4), 443–455. <https://doi.org/10.1080/17512433.2017.1292849>
- Madisen, L., Zwingman, T. A., Sunkin, S. M., Oh, S. W., Zariwala, H. A., Gu, H., Ng, L. L., Palmiter, R. D., Hawrylycz, M. J., Jones, A. R., Lein, E. S., & Zeng, H. (2010). A robust and high-throughput Cre reporting and characterization system for the whole mouse brain. *Nature Neuroscience*, 13(1), 133–140. <https://doi.org/10.1038/nrn.2467>
- Maresz, K., Pryce, G., Ponomarev, E. D., Marsicano, G., Croxford, J. L., Shriver, L. P., Ledent, C., Cheng, X., Carrier, E. J., Mann, M. K., Giovannoni, G., Pertwee, R. G., Yamamura, T., Buckley, N. E., Hillard, C. J., Lutz, B., Baker, D., & Dittell, B. N. (2007). Direct suppression of CNS autoimmune inflammation via the cannabinoid receptor CB1 on neurons and CB2 on autoreactive T cells. *Nature Medicine*, 13(4), 492–497. <https://doi.org/10.1038/nm1561>
- McLane, L. E., Bourne, J. N., Evangelou, A. V., Khandker, L., Macklin, W. B., & Wood, T. L. (2017). Loss of tuberous sclerosis Complex1 in adult oligodendrocyte progenitor cells enhances axon remyelination and increases myelin thickness after a focal demyelination. *The Journal of Neuroscience*, 37(31), 7534–7546. <https://doi.org/10.1523/JNEUROSCI.3454-16.2017>
- McMurrin, C. E., Jones, C. A., Fitzgerald, D. C., & Franklin, R. J. (2016). CNS remyelination and the innate immune system. *Frontiers in Cell and Development Biology*, 4, 38. <https://doi.org/10.3389/fcell.2016.00038>
- Messina, S., Solaro, C., Righini, I., Bergamaschi, R., Bonavita, S., Bossio, R. B., Brescia Morra, V., Costantino, G., Cavalla, P., Centonze, D., Comi, G., Cottone, S., Danni, M. C., Francia, A., Gajofatto, A., Gasperini, C., Zaffaroni, M., Petrucci, L., Signoriello, E., ... S.A.F.E. study group. (2017). Sativex in resistant multiple sclerosis spasticity: Discontinuation study in a large population of Italian patients (S.A.F.E. study). *PLoS ONE*, 12(8), e0180651. <https://doi.org/10.1371/journal.pone.0180651>
- Metna-Laurent, M., Mondesir, M., Grel, A., Vallee, M., & Piazza, P. V. (2017). Cannabinoid-induced tetrad in mice. *Current Protocols in Neuroscience*, 80, 9–59. <https://doi.org/10.1002/cpns.31>
- Micu, I., Plemel, J. R., Capriarello, A. V., Nave, K. A., & Stys, P. K. (2018). Axi-myelinic neurotransmission: A novel mode of cell signalling in the central nervous system. *Nature Reviews. Neuroscience*, 19(1), 49–58. <https://doi.org/10.1038/nrn.2017.128>



- Miron, V. E. (2017). Microglia-driven regulation of oligodendrocyte lineage cells, myelination, and remyelination. *Journal of Leukocyte Biology*, 101(5), 1103–1108. <https://doi.org/10.1189/jlb.3R1116-494R>
- Mobius, W., Cooper, B., Kaufmann, W. A., Imig, C., Ruhwedel, T., Snaidero, N., Saab, A. S., & Varoqueaux, F. (2010). Electron microscopy of the mouse central nervous system. *Methods in Cell Biology*, 96, 475–512. [https://doi.org/10.1016/S0091-679X\(10\)96020-2](https://doi.org/10.1016/S0091-679X(10)96020-2)
- Molina-Gonzalez, I., & Miron, V. E. (2019). Astrocytes in myelination and remyelination. *Neuroscience Letters*, 713, 134532. <https://doi.org/10.1016/j.neulet.2019.134532>
- Molina-Holgado, E., Vela, J. M., Arevalo-Martin, A., Almazan, G., Molina-Holgado, F., Borrell, J., & Guaza, C. (2002). Cannabinoids promote oligodendrocyte progenitor survival: Involvement of cannabinoid receptors and phosphatidylinositol-3 kinase/Akt signaling. *The Journal of Neuroscience*, 22(22), 9742–9753. Retrieved from <https://www.ncbi.nlm.nih.gov/pubmed/12427829>
- Morell, P., Barrett, C. V., Mason, J. L., Toews, A. D., Hostettler, J. D., Knapp, G. W., & Matsushima, G. K. (1998). Gene expression in brain during cuprizone-induced demyelination and remyelination. *Molecular and Cellular Neurosciences*, 12(4–5), 220–227. <https://doi.org/10.1006/mcne.1998.0715>
- Moreno-Luna, R., Esteban, P. F., Paniagua-Torija, B., Arevalo-Martin, A., Garcia-Ovejero, D., & Molina-Holgado, E. (2020). Heterogeneity of the endocannabinoid system between cerebral cortex and spinal cord oligodendrocytes. *Molecular Neurobiology*, 58, 689–702. <https://doi.org/10.1007/s12035-020-02148-1>
- Moreno-Martet, M., Feliu, A., Espejo-Porras, F., Mecha, M., Carrillo-Salinas, F. J., Fernandez-Ruiz, J., Guaza, C., & de Lago, E. (2015). The disease-modifying effects of a Sativex-like combination of phytocannabinoids in mice with experimental autoimmune encephalomyelitis are preferentially due to Delta9-tetrahydrocannabinol acting through CB1 receptors. *Multiple Sclerosis and Related Disorders*, 4(6), 505–511. <https://doi.org/10.1016/j.msard.2015.08.001>
- Morrison, B. M., Lee, Y., & Rothstein, J. D. (2013). Oligodendroglia: Metabolic supporters of axons. *Trends in Cell Biology*, 23(12), 644–651. <https://doi.org/10.1016/j.tcb.2013.07.007>
- Palazuelos, J., Aguado, T., Pazos, M. R., Julien, B., Carrasco, C., Resel, E., Sagredo, O., Benito, C., Romero, J., Azcoitia, I., Fernández-Ruiz, J., Guzmán, M., & Galve-Roperh, I. (2009). Microglial CB2 cannabinoid receptors are neuroprotective in Huntington's disease excitotoxicity. *Brain*, 132(Pt 11), 3152–3164. <https://doi.org/10.1093/brain/awp239>
- Palazuelos, J., Davoust, N., Julien, B., Hatterer, E., Aguado, T., Mechoulam, R., Benito, C., Romero, J., Silva, A., Guzmán, M., Nataf, S., & Galve-Roperh, I. (2008). The CB(2) cannabinoid receptor controls myeloid progenitor trafficking: Involvement in the pathogenesis of an animal model of multiple sclerosis. *The Journal of Biological Chemistry*, 283(19), 13320–13329. <https://doi.org/10.1074/jbc.M707960200>
- Palazuelos, J., Klingener, M., & Aguirre, A. (2014). TGFbeta signaling regulates the timing of CNS myelination by modulating oligodendrocyte progenitor cell cycle exit through SMAD3/4/FoxO1/Sp1. *The Journal of Neuroscience*, 34(23), 7917–7930. <https://doi.org/10.1523/JNEUROSCI.0363-14.2014>
- Palazuelos, J., Klingener, M., Raines, E. W., Crawford, H. C., & Aguirre, A. (2015). Oligodendrocyte regeneration and CNS remyelination require TACE/ADAM17. *The Journal of Neuroscience*, 35(35), 12241–12247. <https://doi.org/10.1523/JNEUROSCI.3937-14.2015>
- Percie du Sert, N., Hurst, V., Ahluwalia, A., Alam, S., Avey, M. T., Baker, M., Browne, W. J., Clark, A., Cuthill, I. C., Dirnagl, U., Emerson, M., Garner, P., Holgate, S. T., Howells, D. W., Karp, N. A., Lázic, S. E., Lidster, K., MacCallum, C. J., Macleod, M., ... Würbel, H. (2020). The ARRIVE guidelines 2.0: Updated guidelines for reporting animal research. *PLoS Biology*, 18(7), e3000410. <https://doi.org/10.1371/journal.pbio.3000410>
- Prut, L., & Belzung, C. (2003). The open field as a paradigm to measure the effects of drugs on anxiety-like behaviors: A review. *European Journal of Pharmacology*, 463(1–3), 3–33. [https://doi.org/10.1016/S0014-2999\(03\)01272-x](https://doi.org/10.1016/S0014-2999(03)01272-x)
- Pryce, G., Ahmed, Z., Hankey, D. J., Jackson, S. J., Croxford, J. L., Pocock, J. M., Ledent, C., Petzold, A., Thompson, A. J., Giovannoni, G., Cuzner, M. L., & Baker, D. (2003). Cannabinoids inhibit neurodegeneration in models of multiple sclerosis. *Brain*, 126(Pt 10), 2191–2202. <https://doi.org/10.1093/brain/awg224>
- Pryce, G., Riddall, D. R., Selwood, D. L., Giovannoni, G., & Baker, D. (2015). Neuroprotection in experimental autoimmune encephalomyelitis and progressive multiple sclerosis by cannabis-based cannabinoids. *Journal of Neuroimmune Pharmacology*, 10(2), 281–292. <https://doi.org/10.1007/s11481-014-9575-8>
- Rizzo, M. D., Henriquez, J. E., Blevins, L. K., Bach, A., Crawford, R. B., & Kaminski, N. E. (2020). Targeting cannabinoid receptor 2 on peripheral leukocytes to attenuate inflammatory mechanisms implicated in HIV-associated neurocognitive disorder. *Journal of Neuroimmune Pharmacology*, 15, 780–793. <https://doi.org/10.1007/s11481-020-09918-7>
- Russo, E. B. (2011). Taming THC: Potential cannabis synergy and phytocannabinoid-terpenoid entourage effects. *British Journal of Pharmacology*, 163(7), 1344–1364. <https://doi.org/10.1111/j.1476-5381.2011.01238.x>
- Sachs, H. H., Bercury, K. K., Popescu, D. C., Narayanan, S. P., & Macklin, W. B. (2014). A new model of cuprizone-mediated demyelination/remyelination. *ASN Neuro*, 6(5), 175909141455195. <https://doi.org/10.1177/1759091414551955>
- Serra-de-Oliveira, N., Boilesen, S. N., Prado de Franca Carvalho, C., LeSueur-Maluf, L., Zollner Rde, L., Spadari, R. C., Medalha, C. C., & Monteiro de Castro, G. (2015). Behavioural changes observed in demyelination model shares similarities with white matter abnormalities in humans. *Behavioural Brain Research*, 287, 265–275. <https://doi.org/10.1016/j.bbr.2015.03.038>
- Shelestak, J., Singhal, N., Frankle, L., Tomor, R., Sternbach, S., McDonough, J., Freeman, E., & Clements, R. (2020). Increased blood-brain barrier hyperpermeability coincides with mast cell activation early under cuprizone administration. *PLoS ONE*, 15(6), e0234001. <https://doi.org/10.1371/journal.pone.0234001>
- Skripuletz, T., Miller, E., Moharreggh-Khiabani, D., Blank, A., Pul, R., Gudi, V., Trebst, C., & Stangel, M. (2010). Beneficial effects of minocycline on cuprizone induced cortical demyelination. *Neurochemical Research*, 35(9), 1422–1433. <https://doi.org/10.1007/s11064-010-0202-7>
- Spitzer, S., Volbracht, K., Lundgaard, I., & Karadottir, R. T. (2016). Glutamate signalling: A multifaceted modulator of oligodendrocyte lineage cells in health and disease. *Neuropharmacology*, 110(Pt B), 574–585. <https://doi.org/10.1016/j.neuropharm.2016.06.014>
- Templeton, N., Kivell, B., McCaughey-Chapman, A., Connor, B., & La Flamme, A. C. (2019). Clozapine administration enhanced functional recovery after cuprizone demyelination. *PLoS ONE*, 14(5), e0216113. <https://doi.org/10.1371/journal.pone.0216113>
- Wade, D. T., Robson, P., House, H., Makela, P., & Aram, J. (2003). A preliminary controlled study to determine whether whole-plant cannabis extracts can improve intractable neurogenic symptoms. *Clinical Rehabilitation*, 17(1), 21–29. <https://doi.org/10.1191/0269215503cr581oa>
- Wirguin, I., Mechoulam, R., Breuer, A., Schezen, E., Weidenfeld, J., & Brenner, T. (1994). Suppression of experimental autoimmune encephalomyelitis by cannabinoids. *Immunopharmacology*, 28(3), 209–214. [https://doi.org/10.1016/0162-3109\(94\)90056-6](https://doi.org/10.1016/0162-3109(94)90056-6)
- Wood, T. L., Bercury, K. K., Cifelli, S. E., Mursch, L. E., Min, J., Dai, J., & Macklin, W. B. (2013). mTOR: A link from the extracellular milieu to transcriptional regulation of oligodendrocyte development. *ASN Neuro*, 5(1), e00108. <https://doi.org/10.1042/AN20120092>



- Xu, H., Yang, H. J., Zhang, Y., Clough, R., Browning, R., & Li, X. M. (2009). Behavioral and neurobiological changes in C57BL/6 mice exposed to cuprizone. *Behavioral Neuroscience*, *123*(2), 418–429. <https://doi.org/10.1037/a0014477>
- Zajicek, J., Ball, S., Wright, D., Vickery, J., Nunn, A., Miller, D., Cano, M. G., McManus, D., Mallik, S., Hobart, J., & CUPID investigator group. (2013). Effect of dronabinol on progression in progressive multiple sclerosis (CUPID): A randomised, placebo-controlled trial. *Lancet Neurology*, *12*(9), 857–865. [https://doi.org/10.1016/S1474-4422\(13\)70159-5](https://doi.org/10.1016/S1474-4422(13)70159-5)
- Zhang, J., Kramer, E. G., Mahase, S., Dutta, D. J., Bonnamain, V., Argaw, A. T., & John, G. R. (2011). Targeting oligodendrocyte protection and remyelination in multiple sclerosis. *Mount Sinai Journal of Medicine*, *78*(2), 244–257. <https://doi.org/10.1002/msj.20244>
- Zhang, M., Zhan, X. L., Ma, Z. Y., Chen, X. S., Cai, Q. Y., & Yao, Z. X. (2015). Thyroid hormone alleviates demyelination induced by cuprizone through its role in remyelination during the remission period. *Experimental Biology and Medicine* (Maywood, N.J.), *240*(9), 1183–1196. <https://doi.org/10.1177/1535370214565975>
- Zhu, X., Bergles, D. E., & Nishiyama, A. (2008). NG2 cells generate both oligodendrocytes and gray matter astrocytes. *Development*, *135*(1), 145–157. <https://doi.org/10.1242/dev.004895>

## SUPPORTING INFORMATION

Additional supporting information may be found online in the Supporting Information section at the end of this article.

**How to cite this article:** Aguado, T., Hueriga-Gómez, A., Sánchez-de la Torre, A., Resel, E., Chara, J. C., Matute, C., Mato, S., Galve-Roperh, I., Guzman, M., & Palazuelos, J. (2021).  $\Delta^2$ -Tetrahydrocannabinol promotes functional remyelination in the mouse brain. *British Journal of Pharmacology*, *178*(20), 4176–4192. <https://doi.org/10.1111/bph.15608>